Measurements of Higgs boson properties with $H \to ZZ \to 4\ell$ and $H \to \gamma\gamma$ at CMS

-- cross sections and mass

Junquan Tao（IHEP/CAS）

陶军全 （中科院高能所）

中国科学院高能物理研究所
Institute of High Energy Physics
Chinese Academy of Sciences

中国物理学会高能物理分会第十一届全国会员代表大会暨学术年会

2022年8月8日至11日,大连

Introduction

- At the LHC, H→ZZ→4ℓ and H→ γγ are two of the most important channels first in the **discovery of the Higgs boson**, and then in the **measurements of Higgs boson properties** and also in **searches for new physics**
  - Final state, μ/e/γ, can be **fully reconstructed** with **excellent mass resolution (about** 1-2%**)**
- **H→ZZ→4ℓ : Large signal-to-background ratio, " the golden channel"**
  - Tiny signal yield due to small ZZ → 4ℓ BR
  - A low background rate, mainly from non-resonant ZZ
- **H→γγ : search for a narrow peak on a larger falling background in mass distribution**
  - Small signal yield due to tiny BR (0.2%)
  - Large backgrounds including continuum γγ (irreducible) and fakes from γj and jj (reducible)
  - Loop-induced decay: new physics could contribute to the loop

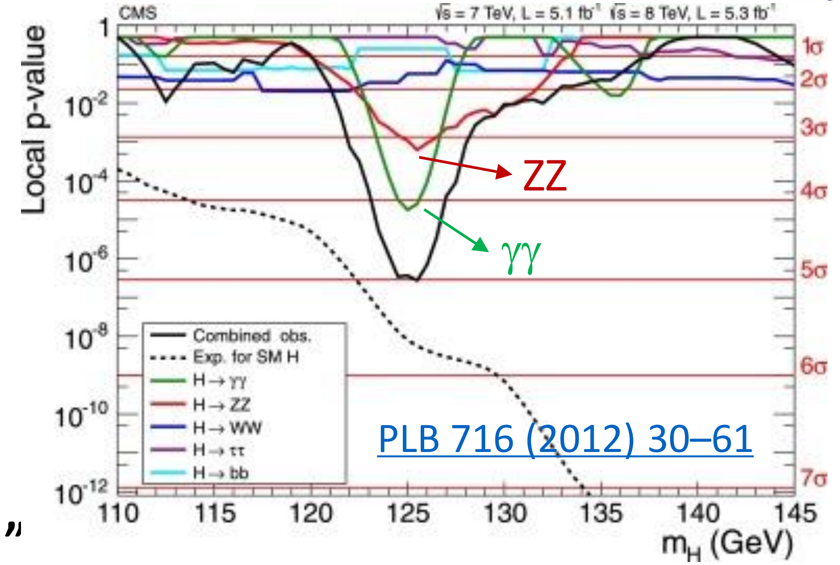

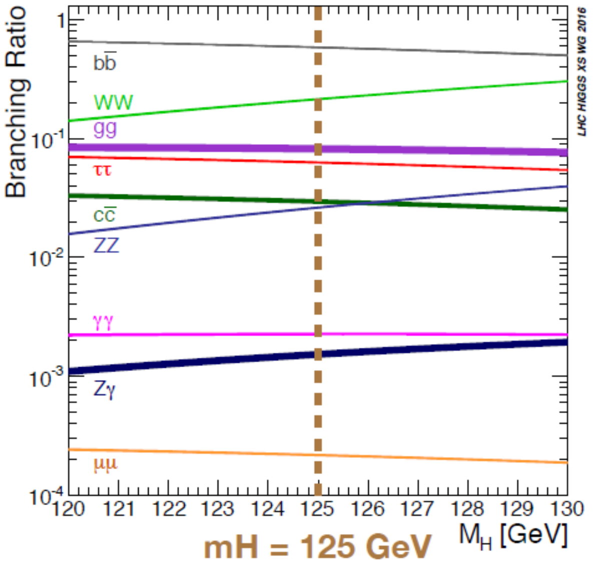

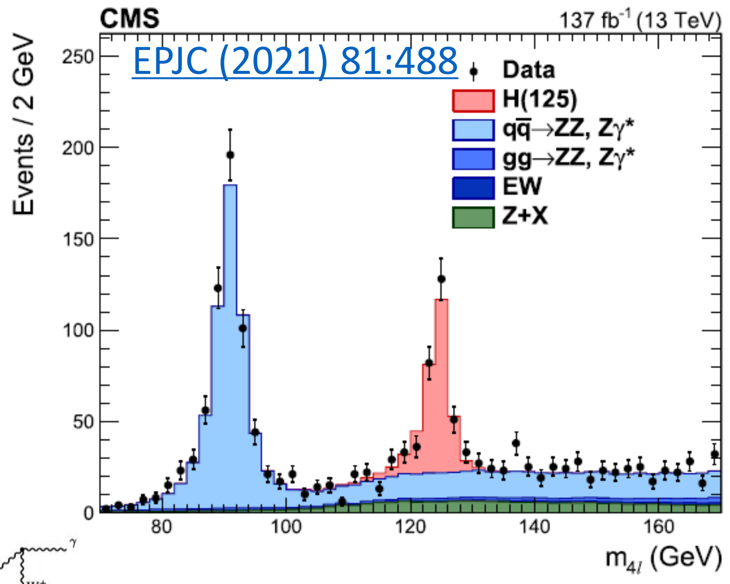

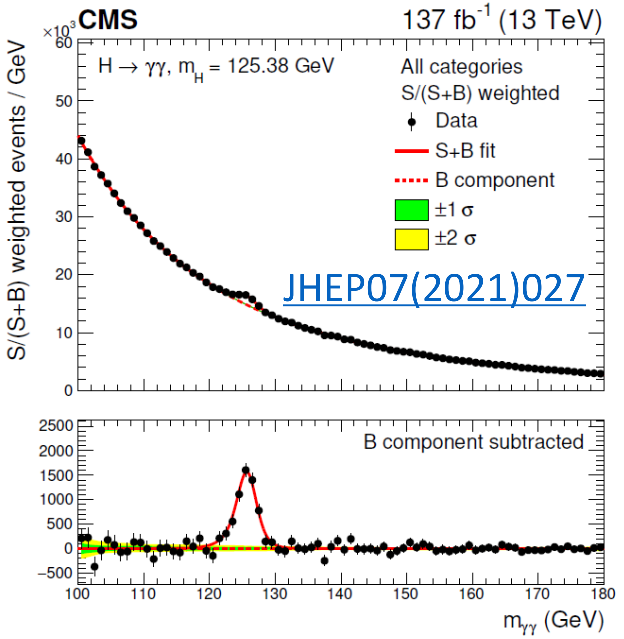

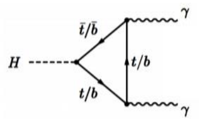

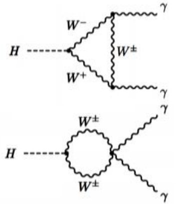

In this talk

Some latest results of Higgs boson properties from $H \to ZZ \to 4\ell$ and $H \to \gamma\gamma$ at CMS, including

- **(Inclusive) cross section or signal strength**
- **Simplified template cross sections (STXS)**
- **Fiducial and differential cross sections**
- **Higgs mass measurements and projections at the HL-LHC**

Also see more CMS Higgs boson property results from:

Jin Wang, "Combined measurement of Higgs properties"
Li Yuan, "Measurement of the Higgs boson width in ZZ final states at CMS"
Chaochen Yuan, "CP violation in ttH and tH in multilepton channels (includes combination) at CMS"
Yuekai Song, "Measurement of top-Yukawa CP and Higgs EFT in ZZ and tautau final states at CMS"
Congqiao Li, "Search for Higgs boson decay to a charm quark-antiquark pair in proton-proton collisions at sqrt(s) = 13 TeV at CMS"
…

H→ZZ→ 4ℓ : analysis overview

- **Three final states** are considered separately : 4μ, 4e and 2μ2e
  - FSR photons are included in invariant mass computations
  - Z candidates： pairs of leptons of the same flavor and opposite-charge; “Z_1 ” the Z candidate with an invariant mass closest to the nominal Z boson mass

- **Background estimations**: gg→ZZ and qq→ZZ from simulation, Z+X from data

- **Matrix-element kinematic discriminants** for classification
  - Designed to separate the targeted H boson production mode from its dominant background
  - Angular correlations, mass … kinematic information

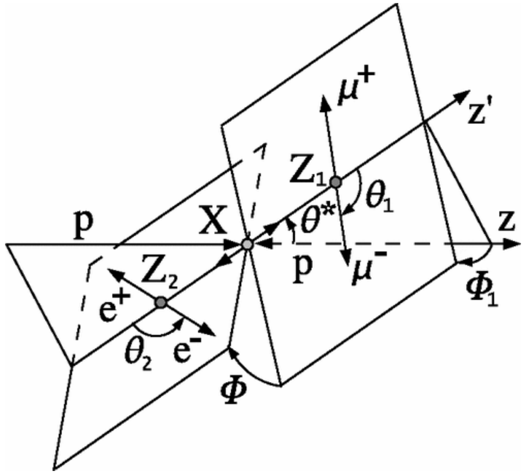

$$\mathcal{D}_{\rm bkg}^{\rm kin} = \left[1 + \frac{\mathcal{P}_{\rm bkg}^{q\bar{q}}(\vec{\Omega}^{\rm H\to 4\ell}|m_{4\ell})}{\mathcal{P}_{\rm sig}^{gg}(\vec{\Omega}^{\rm H\to 4\ell}|m_{4\ell})}\right]^{-1}$$

$$\mathcal{D}_{\rm bkg}^{\rm VBF+dec} = \left[1 + \frac{c^{\rm VBF}(m_{4\ell})[\mathcal{P}_{\rm bkg}^{\rm EW}(\vec{\Omega}^{\rm H+jj}|m_{4\ell}) + \mathcal{P}_{\rm bkg}^{\rm QCD}(\vec{\Omega}^{\rm H+jj}|m_{4\ell})]}{\mathcal{P}_{\rm sig}^{\rm EW}(\vec{\Omega}^{\rm H+jj}|m_{4\ell})}\right]^{-1}$$

$$\mathcal{D}_{\rm bkg}^{\rm VH+dec} = \left[1 + \frac{c^{\rm VH}(m_{4\ell})[\mathcal{P}_{\rm bkg}^{\rm EW}(\vec{\Omega}^{\rm H+jj}|m_{4\ell}) + \mathcal{P}_{\rm bkg}^{\rm QCD}(\vec{\Omega}^{\rm H+jj}|m_{4\ell})]}{\mathcal{P}_{\rm sig}^{\rm EW}(\vec{\Omega}^{\rm H+jj}|m_{4\ell})}\right]^{-1}$$

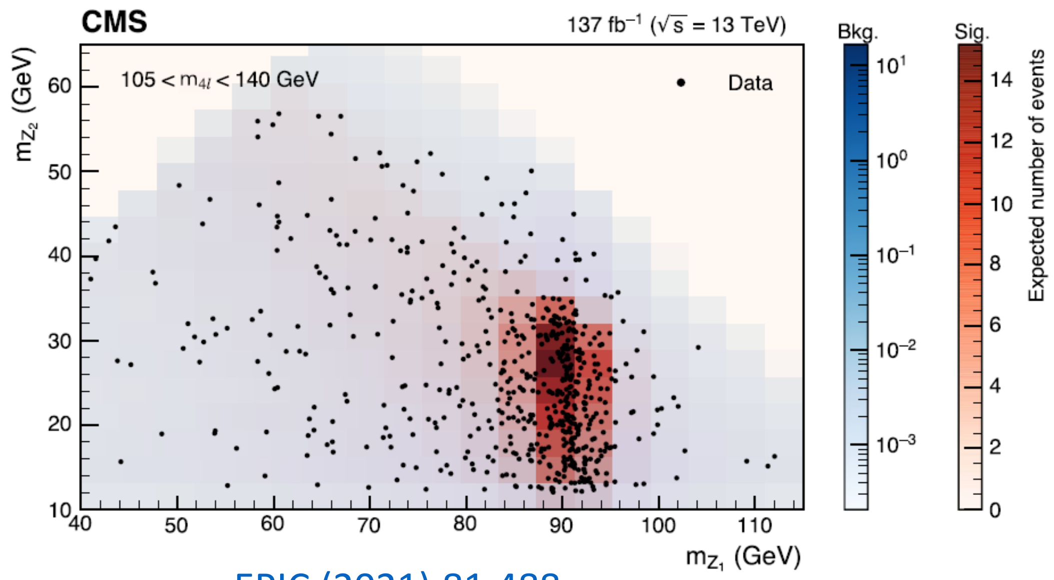

EPJC (2021) 81:488

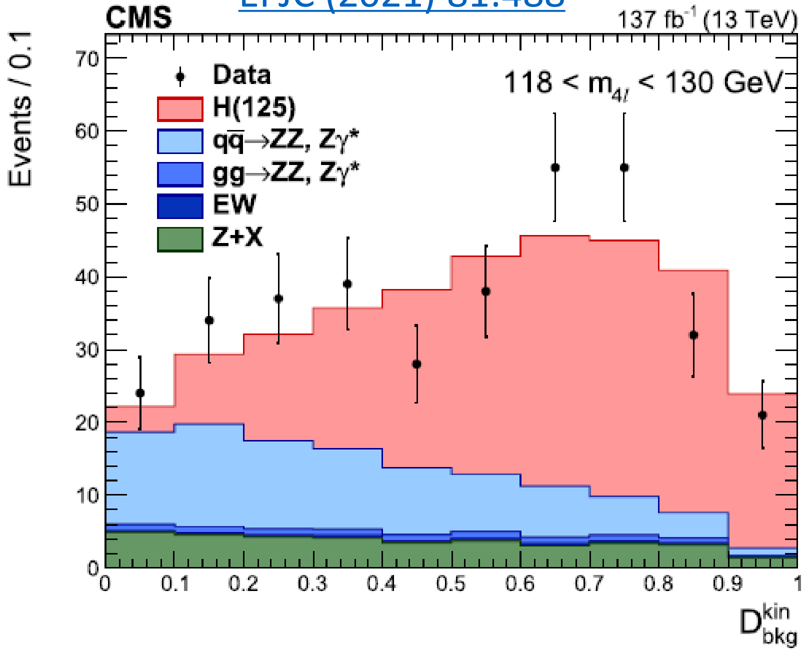

H→γγ: analysis overview

- **To achieve good mass resolution**
  - ✓ select/reconstruct two **photons** with precise **photon energy : MVA *regression*** after calibrations
  - ✓ Find the **primary vertex** of the Higgs decay: ***MVA BDT***

- **Fake photon suppression**: photon identification *BDT* inputs of diphoton BDT after looser cut (>-0.9)

- Several different machine learning (**ML**) algorithms (BDTs, DNNs) are used to **separate signal from background** and reduce the contamination from other H production modes
  - ✓ **Diphoton BDT** based on kinematics including mass resolution (ggH)
  - ✓ Dedicated **selection criteria and classifiers** are used to select events consistent with the tH, ttH, VH, VBF

- **Signal are extracted** by a simultaneous maximum-likelihood fit to the **diphoton mass** in all event classes

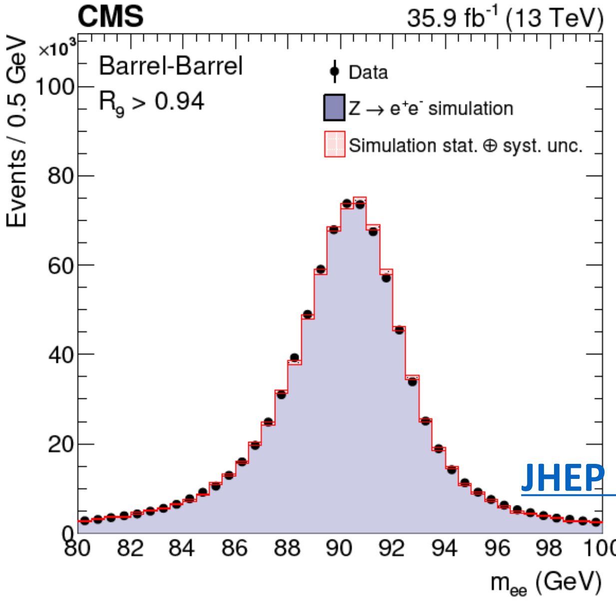

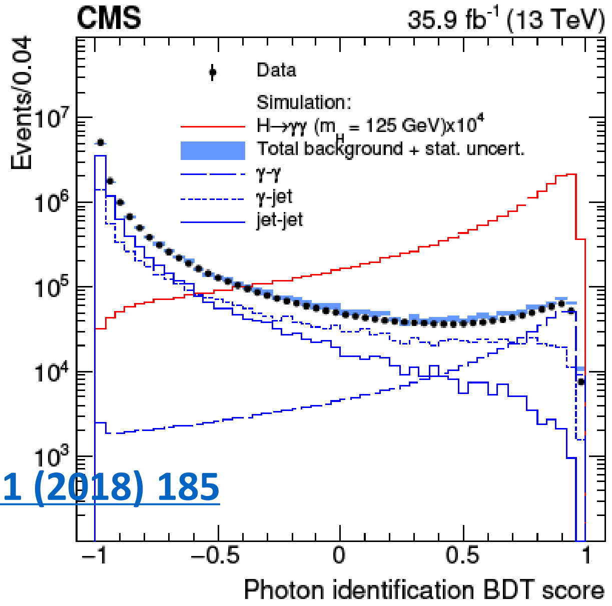

JHEP 11 (2018) 185

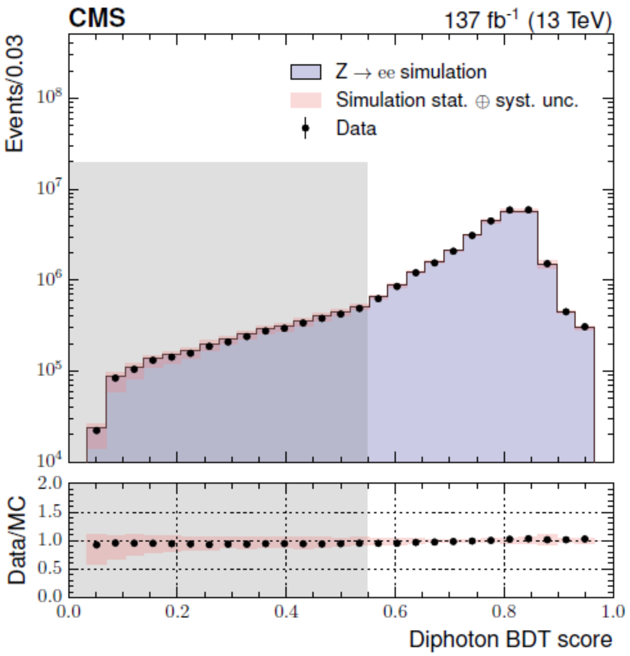

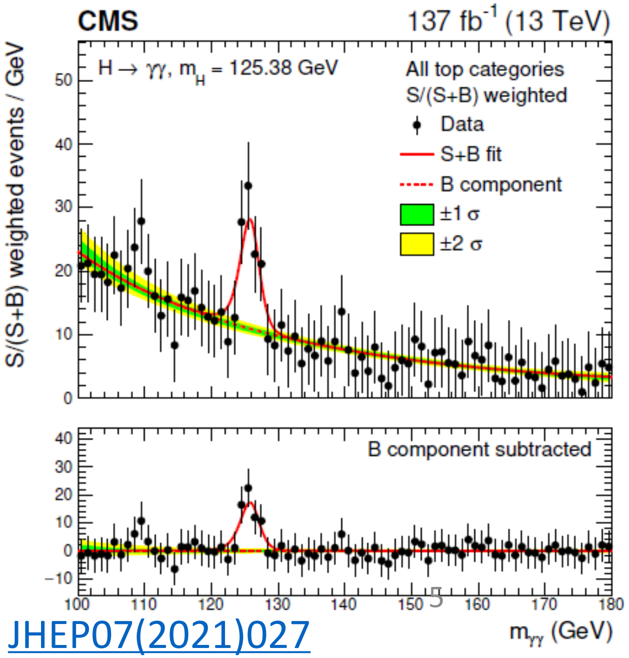

JHEP07(2021)027

(Inclusive) cross sections or signal strength

- First quantity to measure when establishing a channel
- Signal strength modifier (μ) is defined as the ratio between the **measured signal cross section** and the **SM expectation**
- Inclusive signal strength modifier is measured to be

$$\mu_i = \frac{\sigma_i}{\sigma_i^{\mathrm{SM}}} \qquad \mu^f = \frac{\mathcal{B}^f}{\mathcal{B}^f_{\mathrm{SM}}}$$

$$\mu_i^f = \frac{\sigma_i \cdot \mathcal{B}^f}{(\sigma_i \cdot \mathcal{B}^f)_{\mathrm{SM}}} = \mu_i \times \mu^f$$

$\mu = 0.94^{+0.12}_{-0.11} = 0.94 \pm 0.07\,(\mathrm{stat})^{+0.07}_{-0.06}\,(\mathrm{theo})^{+0.06}_{-0.05}\,(\mathrm{exp})$ **(H→ZZ→4l)**

~10% precision

$\mu = 1.12^{+0.09}_{-0.09} = 1.12^{+0.06}_{-0.06}\,(\mathrm{theo})^{+0.03}_{-0.03}\,(\mathrm{syst})^{+0.07}_{-0.06}\,(\mathrm{stat})$ **(H→γγ)**

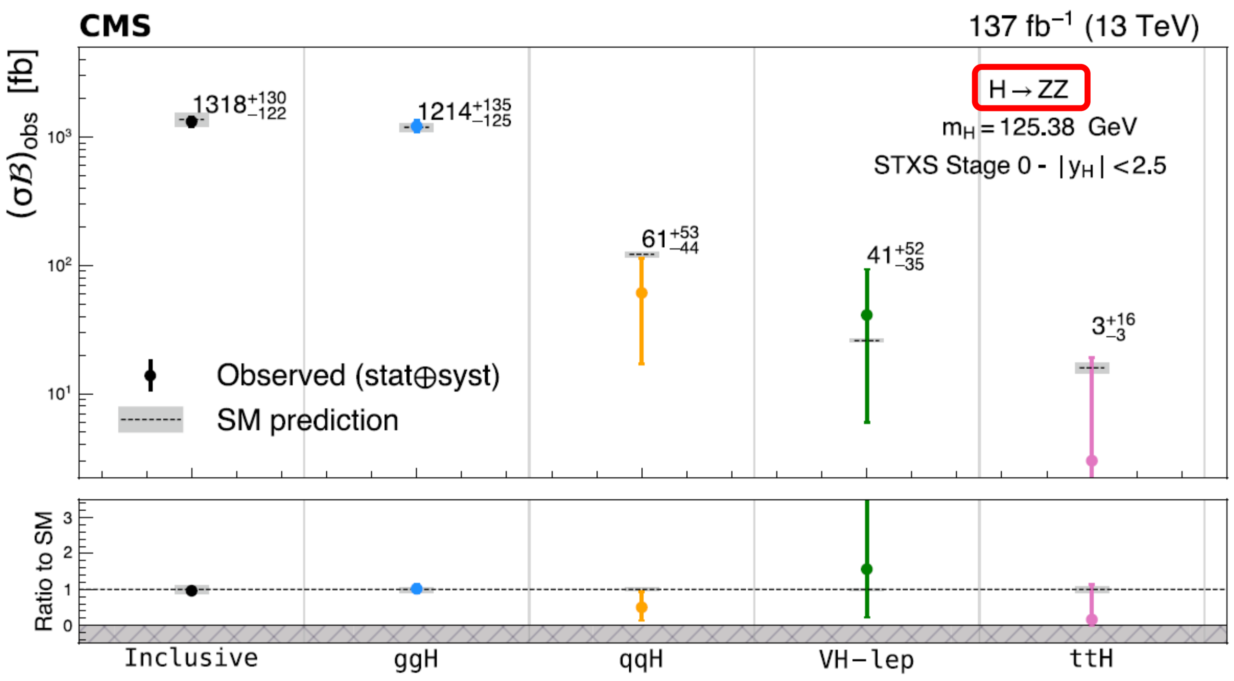

EPJC (2021) 81:488

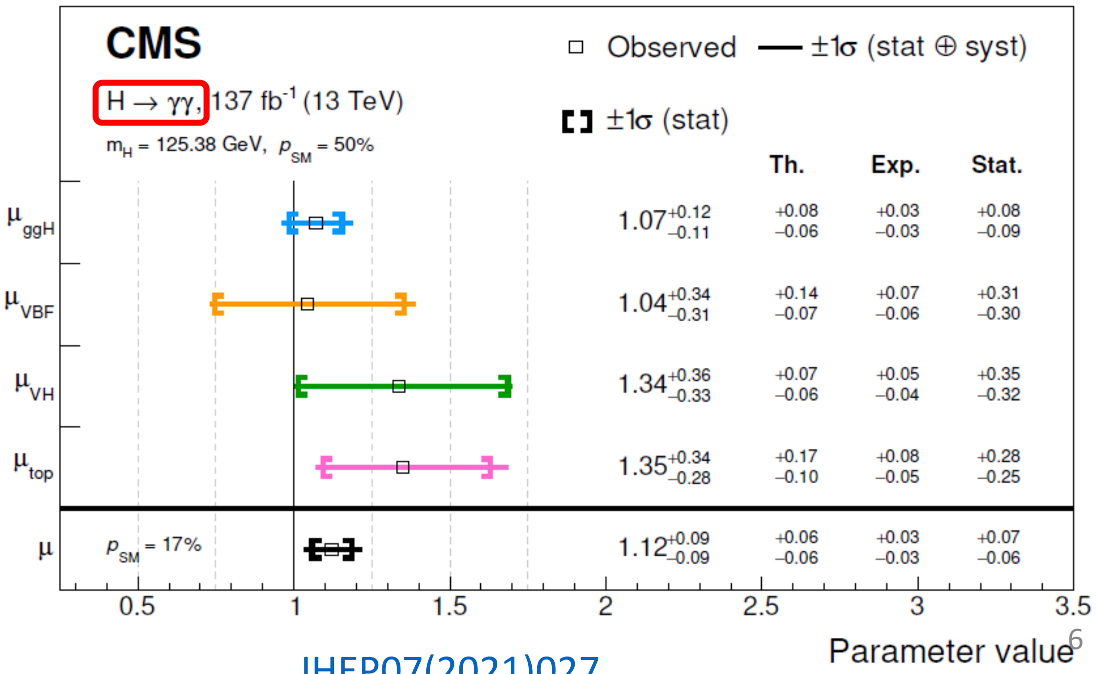

	Value	Th.	Exp.	Stat.
μ_{ggH}	$1.07^{+0.12}_{-0.11}$	$^{+0.08}_{-0.06}$	$^{+0.03}_{-0.03}$	$^{+0.08}_{-0.09}$
μ_{VBF}	$1.04^{+0.34}_{-0.31}$	$^{+0.14}_{-0.07}$	$^{+0.07}_{-0.06}$	$^{+0.31}_{-0.30}$
μ_{VH}	$1.34^{+0.36}_{-0.33}$	$^{+0.07}_{-0.06}$	$^{+0.05}_{-0.04}$	$^{+0.35}_{-0.32}$
μ_{top}	$1.35^{+0.34}_{-0.28}$	$^{+0.17}_{-0.10}$	$^{+0.08}_{-0.05}$	$^{+0.28}_{-0.25}$
μ	$1.12^{+0.09}_{-0.09}$	$^{+0.06}_{-0.06}$	$^{+0.03}_{-0.03}$	$^{+0.07}_{-0.06}$

JHEP07(2021)027

Simplified template cross sections (STXS)

- XS measured in all production processes in several kinematic regimes to **maximize sensitivity** to beyond SM physics **while limiting model dependence**
  - ✓ Target **different production modes** : ggH, qqH (VBF and VH hadronic), VH leptonic, ttH and tH
  - ✓ In each production mode categories are defined to target **as many STXS bins as possible**, according to $p_T(H)$/ $p_T(Hjj)$/$p_T(V)$, N_{jet}, M_{jj}, …
  - ✓ Event categories (proposed production bins) are merged depending on available statistics

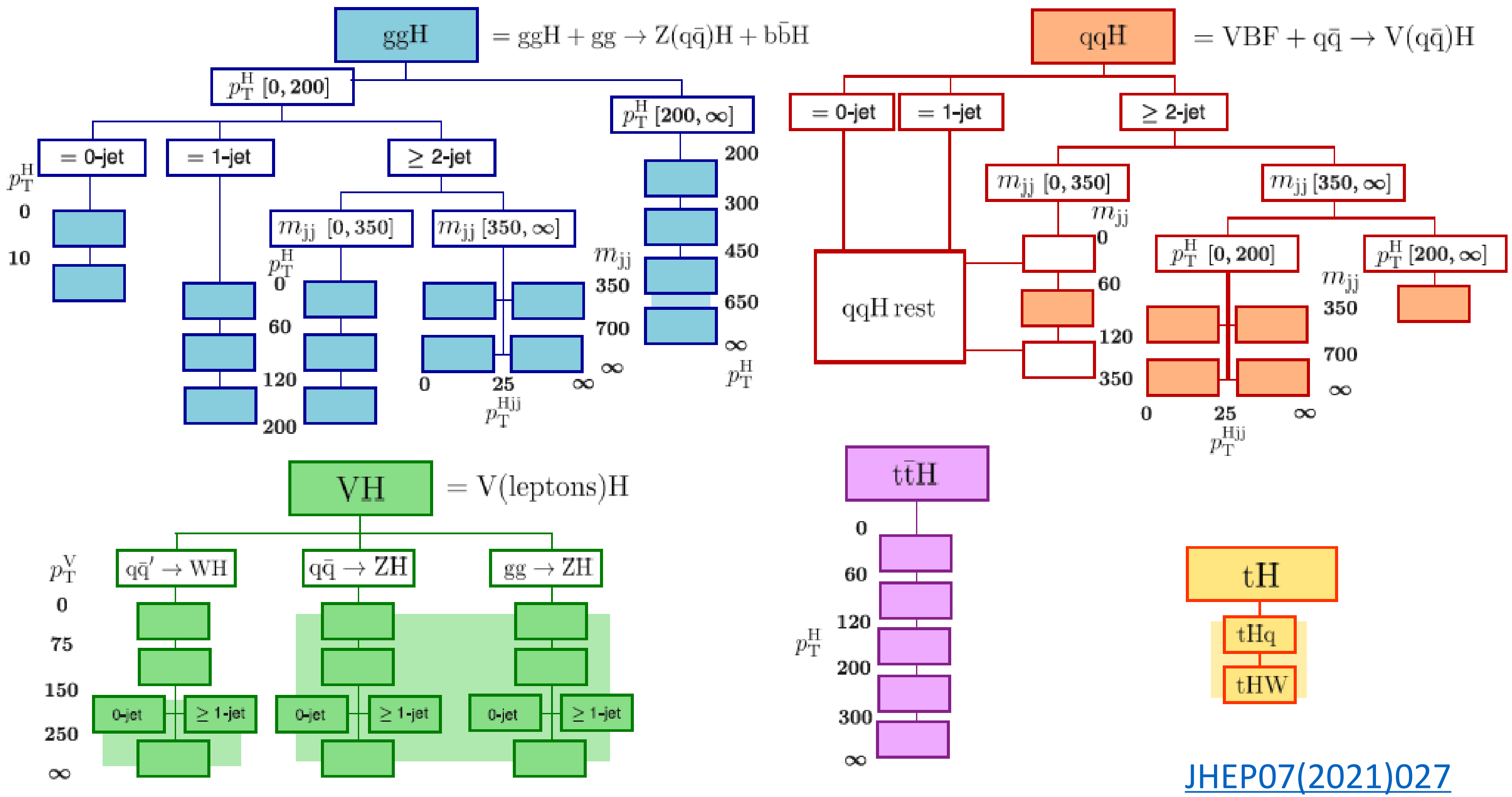

JHEP07(2021)027

Full set of **STXS stage-1.2** bins

H→ZZ→4ℓ STXS

- **19 bins**: ggH (10 bins), qqH (6 bins), VH leptonic (2 bins) and ttH (1 bin)
- $\boldsymbol{\sigma}$ results are consistent, within their uncertainties, with the expectations for the Standard Model H boson

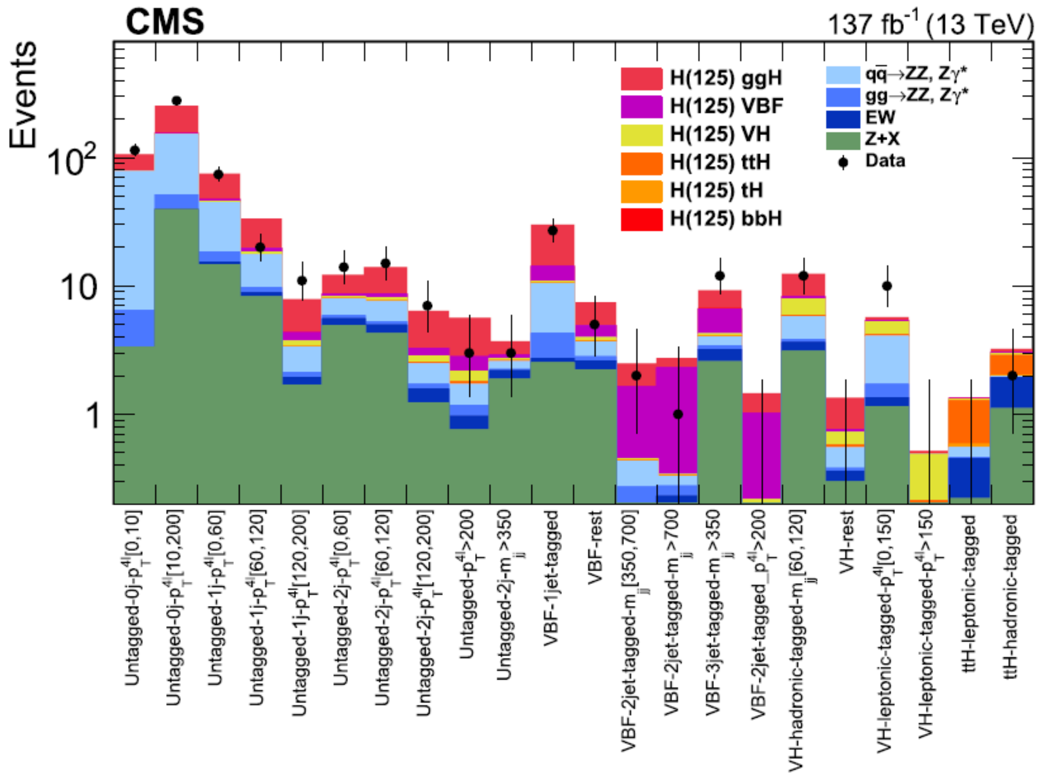

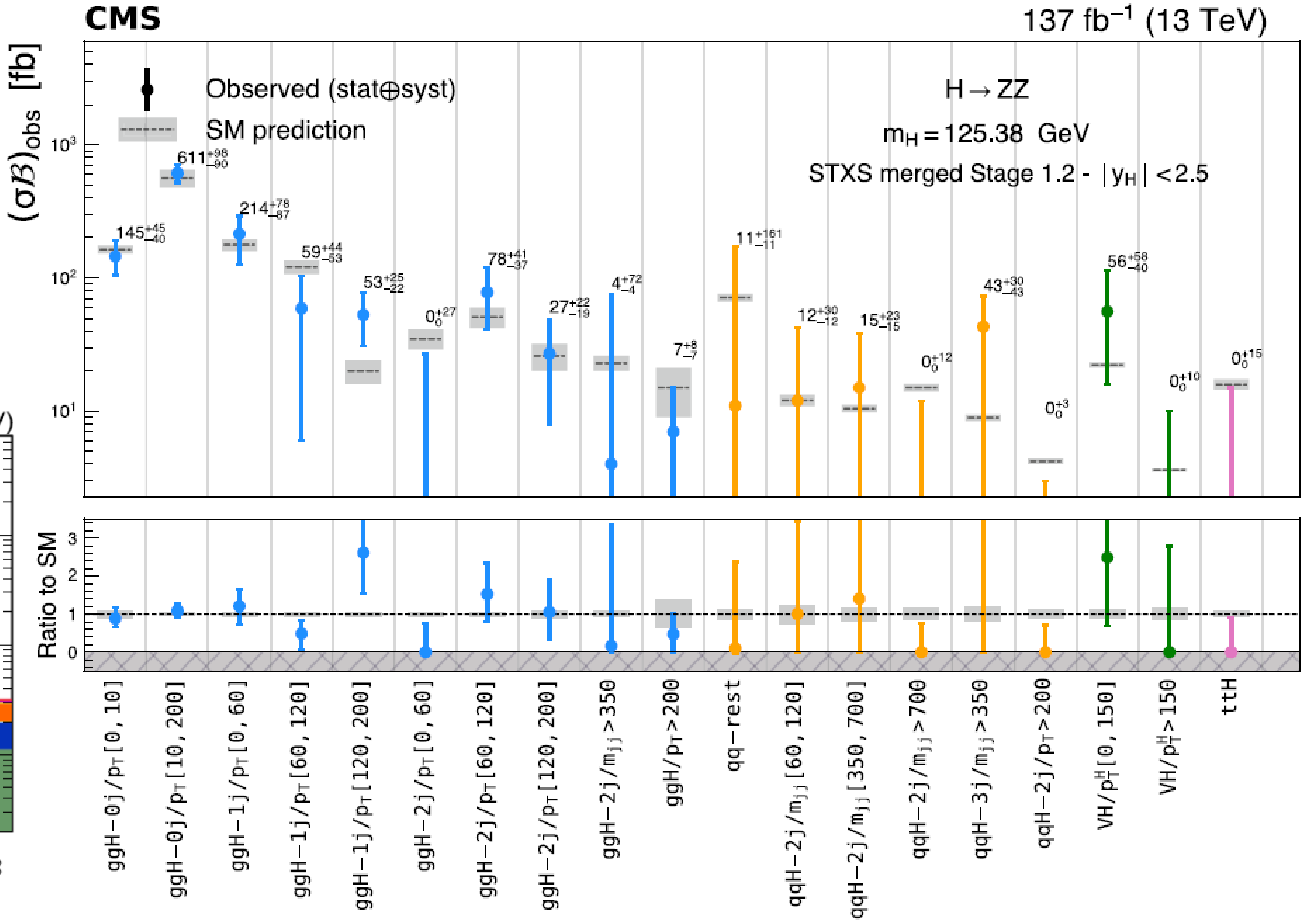

EPJC (2021) 81:488

H→γγ STXS

- **“Maximal” merging scenario (17** POI): STXS bins are merged until their **expected uncertainty is less than 150%** of the SM prediction
  - ✓ Measurement of ttH and tH simultaneously
  - ✓ **First and best tH measurement**: a rate of tH production of 14 (8) times the SM expectation is observed (expected) to be excluded at the 95% CL
  - ✓ BSM bins (in ggH and qqH) : in agreement with SM

- **“Minimal” merging scenario (27** POI): merged as few bins as possible that parameters do **not become too anti-correlated** (less than around 90%)
  - ✓ Additional splitting of ttH (5 bins) and ggH BSM (3 bins)
  - ✓ Merged **ggH** and **VBF** bins: less model dependence and reduced correlations

All $\boldsymbol{\sigma}$ results are in agreement with the SM predictions

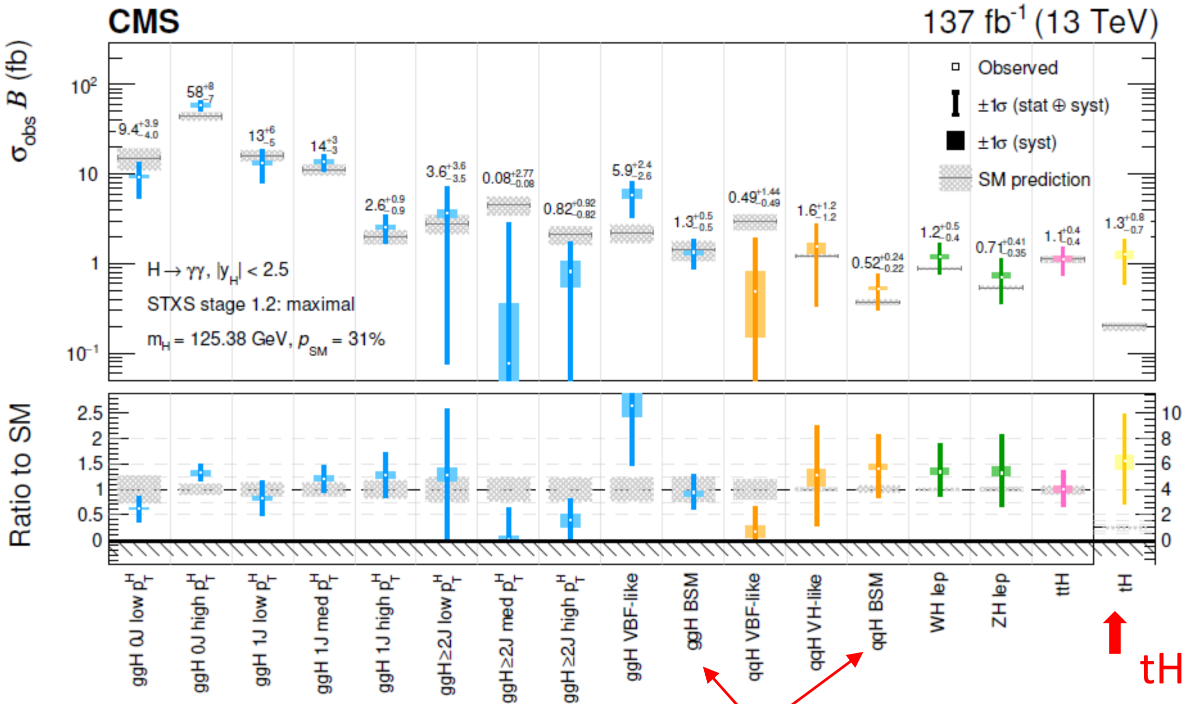

tH

BSM bins

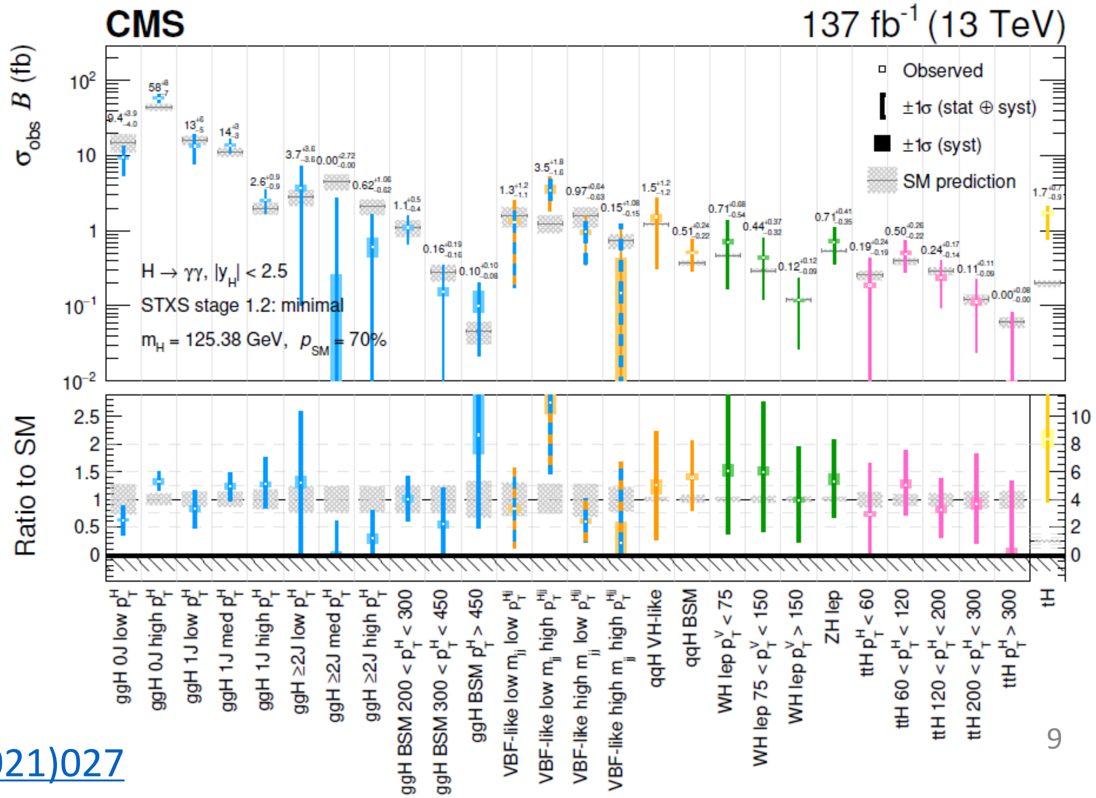

JHEP07(2021)027

Fiducial and differential cross sections

- Fiducial cross sections aim at providing a set of **model independent** results
- Fiducial volume is based on generator-level quantities

Fiducial phase space of $H\to\gamma\gamma$

Observable	Selection
$p_T^{\gamma_1}/m_{\gamma\gamma}$	$> 1/3$
$p_T^{\gamma_2}/m_{\gamma\gamma}$	$> 1/4$
$\mathcal{I}_{gen}^{\gamma}$	$< 10\,\mathrm{GeV}$
$\lvert\eta^{\gamma}\rvert$	< 2.5

EPJC (2021) 81:488

Requirements for the $H \to 4\ell$ fiducial phase space	
Lepton kinematics and isolation	
Leading lepton p_T	$p_T > 20\,\mathrm{GeV}$
Next-to-leading lepton p_T	$p_T > 10\,\mathrm{GeV}$
Additional electrons (muons) p_T	$p_T > 7(5)\,\mathrm{GeV}$
Pseudorapidity of electrons (muons)	$\lvert\eta\rvert < 2.5\ (2.4)$
Sum of scalar p_T of all stable particles within $\Delta R < 0.3$ from lepton	$< 0.35\,p_T$
Event topology	
Existence of at least two same-flavor OS lepton pairs, where leptons satisfy criteria above	
Inv. mass of the Z_1 candidate	$40 < m_{Z_1} < 120\,\mathrm{GeV}$
Inv. mass of the Z_2 candidate	$12 < m_{Z_2} < 120\,\mathrm{GeV}$
Distance between selected four leptons	$\Delta R(\ell_i, \ell_j) > 0.02$ for any $i \neq j$
Inv. mass of any opposite sign lepton pair	$m_{\ell^+\ell'^-} > 4\,\mathrm{GeV}$
Inv. mass of the selected four leptons	$105 < m_{4\ell} < 140\,\mathrm{GeV}$

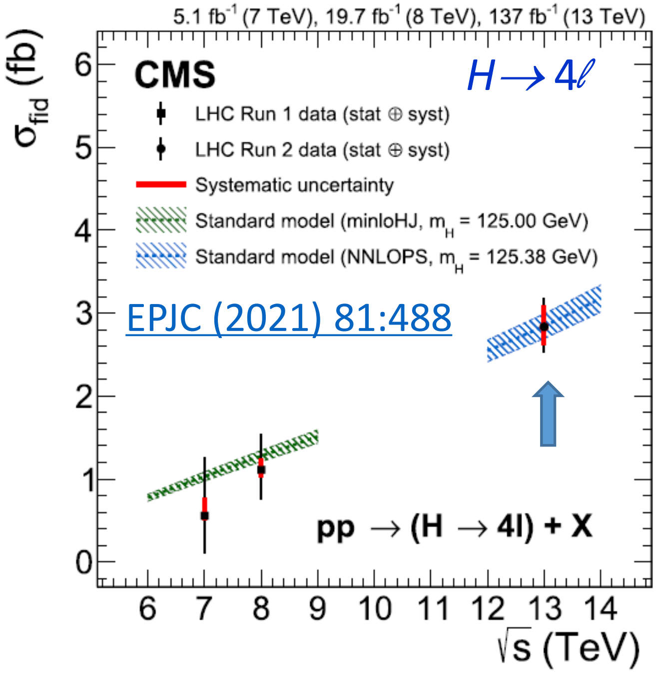

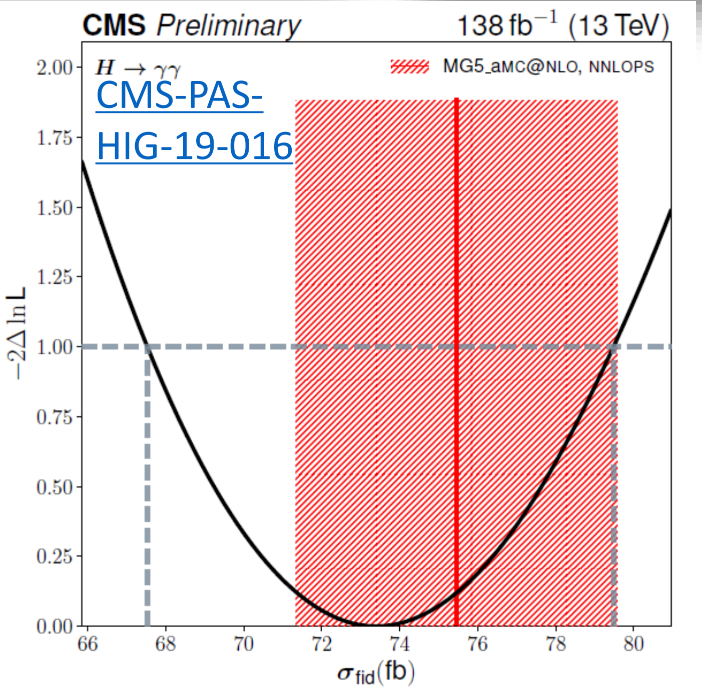

Inclusive fiducial XS

$H\to 4\ell$

$$\sigma_{fid} = 2.84^{+0.34}_{-0.31} = 2.84^{+0.23}_{-0.22}\,(\mathrm{stat})^{+0.26}_{-0.21}\,(\mathrm{syst})\,\mathrm{fb}$$

σ_{fid}=2.84±0.15 fb (SM prediction)

$H\to\gamma\gamma$

$$\sigma_{fid} = 73.40^{+5.4}_{-5.3}(\mathrm{stat})^{+2.4}_{-2.2}(\mathrm{syst})\,\mathrm{fb} = 73.40^{+6.1}_{-5.9}\,\mathrm{fb}$$

σ_{fid}=75.44±4.13 fb (SM prediction)

Fiducial cross sections

H→ ZZ→ 4ℓ fiducial cross section in each year of 2016-2018 and in **different final states**

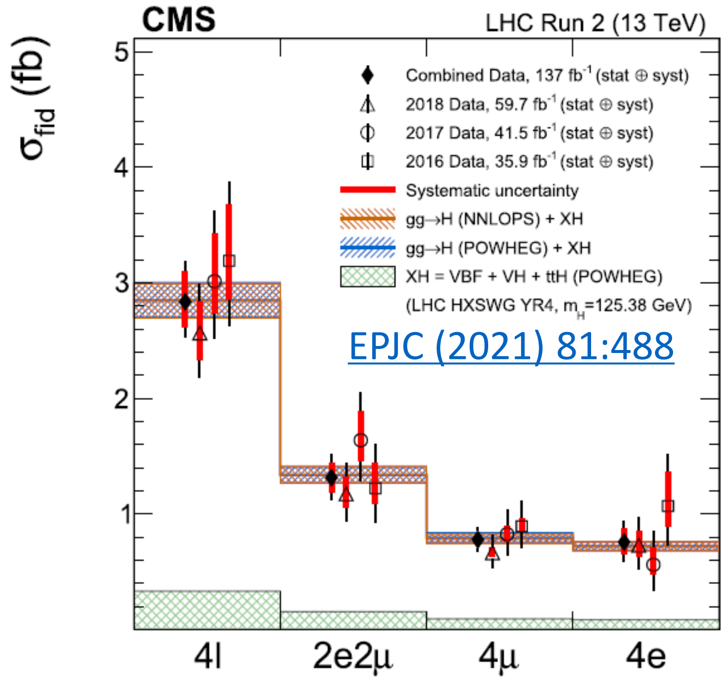

	2e2μ (fb)	4μ (fb)	4e (fb)	Inclusive (fb)
2016	$1.22^{+0.38}_{-0.30}$	$0.89^{+0.22}_{-0.19}$	$1.07^{+0.44}_{-0.33}$	$3.19^{+0.68}_{-0.56} = 3.19^{+0.48}_{-0.45}$ (stat) $^{+0.48}_{-0.33}$ (syst)
2017	$1.64^{+0.41}_{-0.35}$	$0.82^{+0.21}_{-0.18}$	$0.56^{+0.29}_{-0.22}$	$3.01^{+0.60}_{-0.50} = 3.01^{+0.44}_{-0.41}$ (stat) $^{+0.41}_{-0.27}$ (syst)
2018	$1.17^{+0.27}_{-0.24}$	$0.66^{+0.15}_{-0.13}$	$0.73^{+0.24}_{-0.20}$	$2.57^{+0.42}_{-0.38} = 2.57^{+0.33}_{-0.31}$ (stat) $^{+0.27}_{-0.23}$ (syst)
2016–2018	$1.31^{+0.20}_{-0.19}$	$0.78^{+0.10}_{-0.10}$	$0.76^{+0.18}_{-0.16}$	$2.84^{+0.34}_{-0.31} = 2.84^{+0.23}_{-0.22}$ (stat) $^{+0.26}_{-0.21}$ (syst)

H→γγ cross section in **dedicated regions** of the fiducial phase space : selection criteria on top of the fiducial requirements

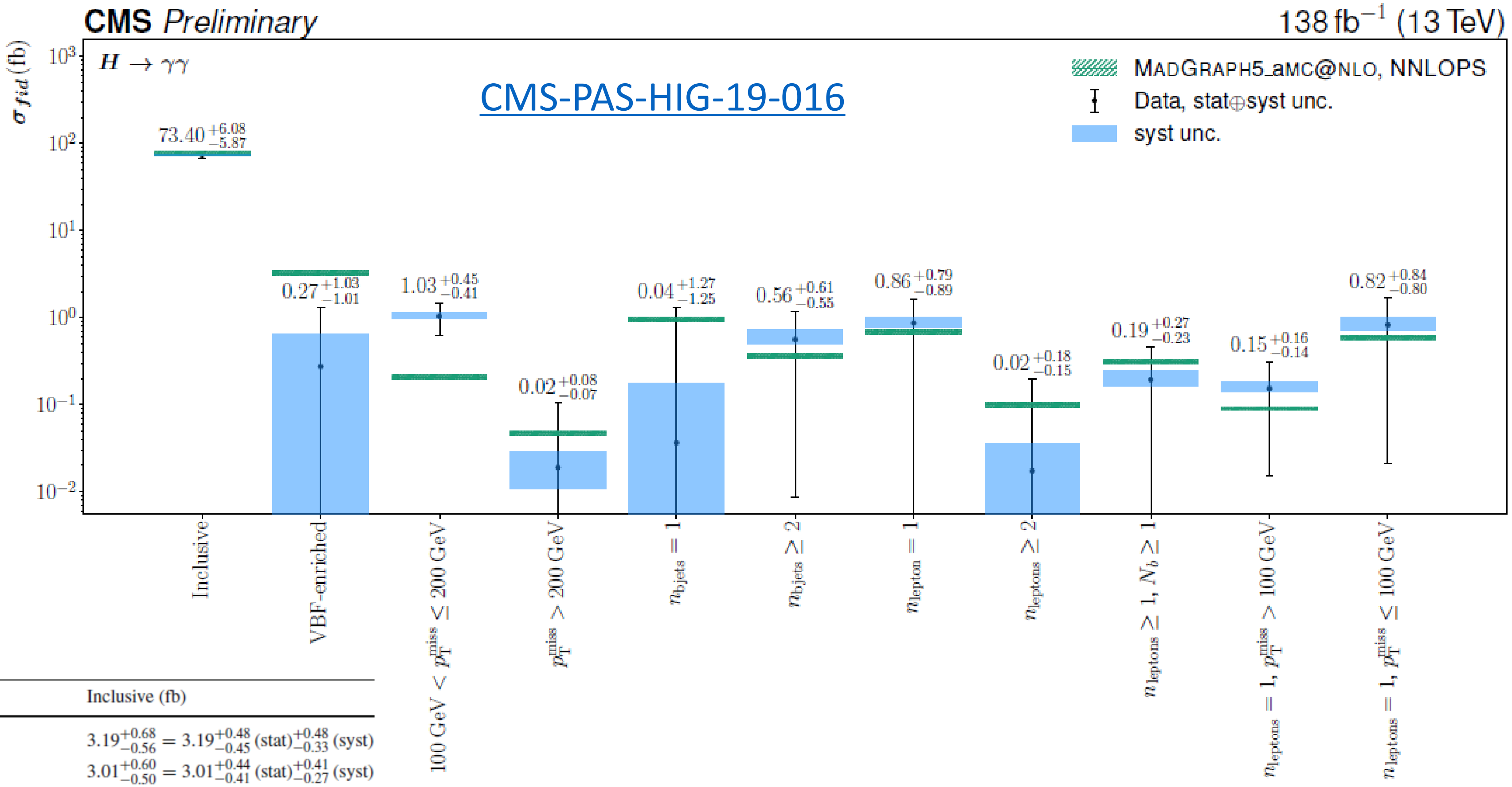

Differential fiducial cross sections

- Differential cross sections of **H→ZZ→ 4ℓ** as a function of p^H_T , H rapidity ($|y_H|$), N_j, and the leading jet (p^j_T)
  -- measurements with more observables with Run2 ultra-legacy data are still ongoing (HIG-21-009)… stay tune!

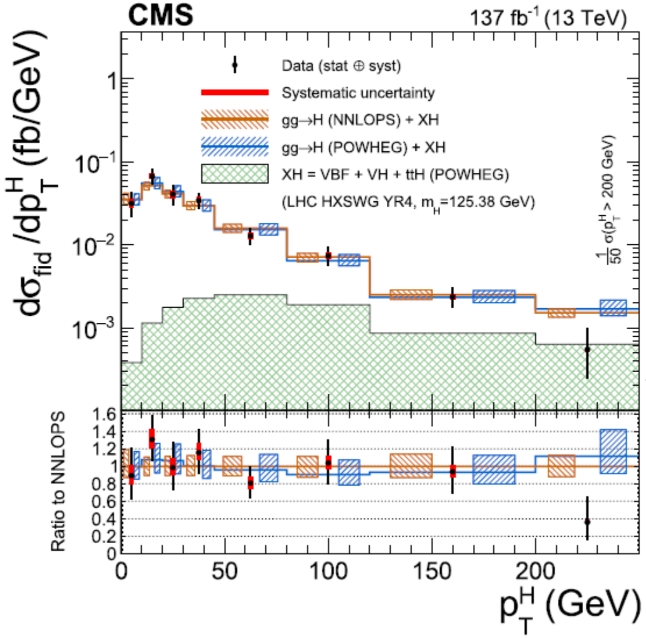

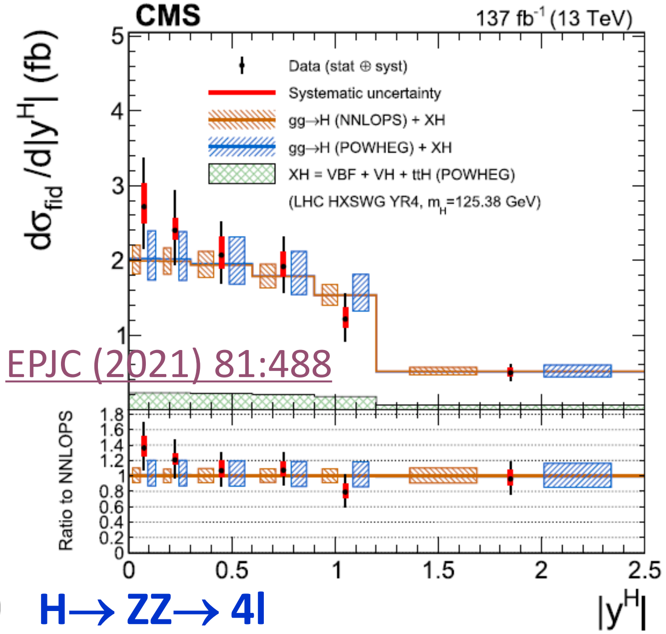

EPJC (2021) 81:488

H→ ZZ→ 4l

- Differential fiducial XS of **H→γγ: large range of variables measured**

Phase Space Region	Observable
Baseline $p_T^{\gamma_1}/m_{\gamma\gamma} > 1/3$ $p_T^{\gamma_2}/m_{\gamma\gamma} > 1/4$ $\lvert\eta^\gamma\rvert < 2.5$ $\mathcal{I}^\gamma_{gen} < 10\,\text{GeV}$	$p_T^{\gamma\gamma}$ n_{jets} $\lvert y^{\gamma\gamma}\rvert$ $\lvert\cos(\theta^*)\rvert$ $\lvert\phi^*_\eta\rvert$ $p_T^{\gamma\gamma}, n_{jets}=0$ $p_T^{\gamma\gamma}, n_{jets}=1$ $p_T^{\gamma\gamma}, n_{jets}>1$ n^b_{jets} $n_{leptons}$ p_T^{miss}
1-jet Baseline + ≥ 1 jet $p_T^j > 30$ GeV $\lvert\eta^j\rvert < 2.5$	$p_T^{j_1}$ $\lvert y^{j_1}\rvert$ $\lvert\Delta\phi_{\gamma\gamma,j_1}\rvert$ $\lvert\Delta y_{\gamma\gamma,j_1}\rvert$ τ^j_C $p_T^{\gamma\gamma}, \tau_{Cj} < 15$ GeV $p_T^{\gamma\gamma}$, 15 GeV $\le \tau^j_C < 25$ GeV $p_T^{\gamma\gamma}$, 25 GeV $\le \tau^j_C < 40$ GeV $p_T^{\gamma\gamma}$, 40 GeV $\le \tau^j_C$
2-jets Baseline + ≥ 2 jets $p_T^j > 30$ GeV $\lvert\eta^j\rvert < 4.7$	$p_T^{j_2}$ $\lvert y^{j_2}\rvert$ $\lvert\Delta\phi_{j_1,j_2}\rvert$ $\lvert\Delta\phi_{\gamma\gamma,j_1j_2}\rvert$ $\lvert\bar\eta_{j_1j_2} - \eta_{\gamma\gamma}\rvert$ m^{jj} $\lvert\Delta\eta_{j_1,j_2}\rvert$
VBF-enriched 2-jets + $n_{jets} \ge 2$ $\Delta\eta^{jj} > 3.5$ $m^{jj} > 200\,\text{GeV}$	$p_T^{\gamma\gamma}$ $p_T^{j_2}$ $\lvert\Delta\phi_{j_1,j_2}\rvert$ $\lvert\Delta\phi_{\gamma\gamma,j_1j_2}\rvert$

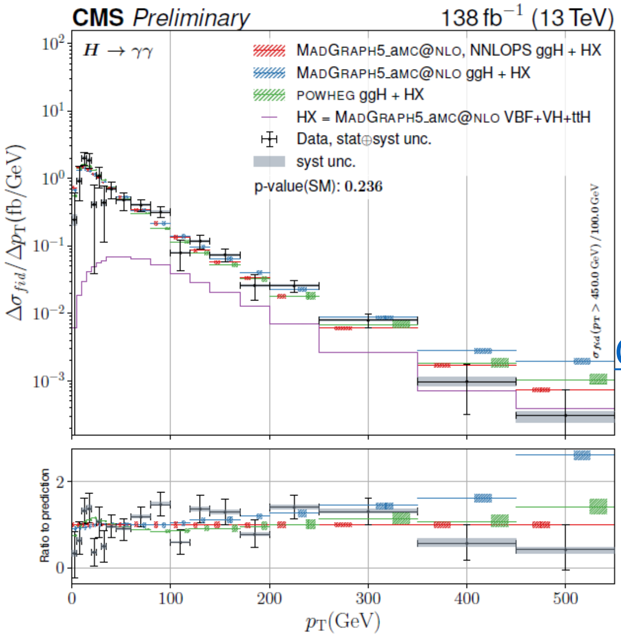

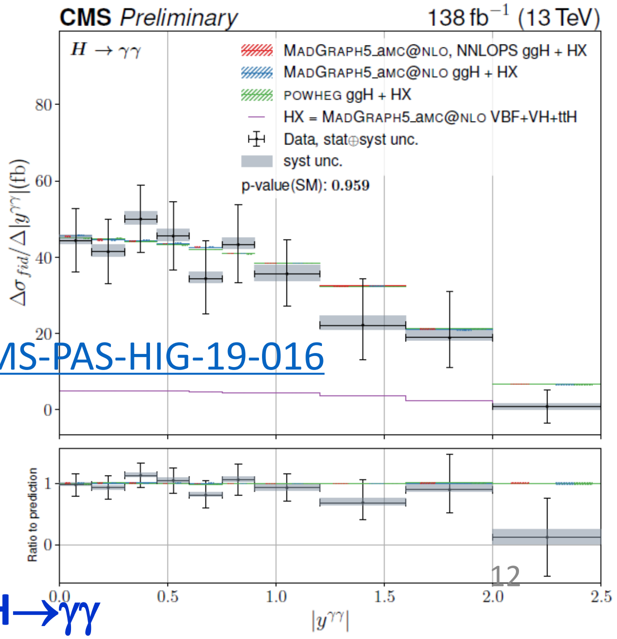

CMS-PAS-HIG-19-016

H→γγ

Differential fiducial cross sections (cont.)

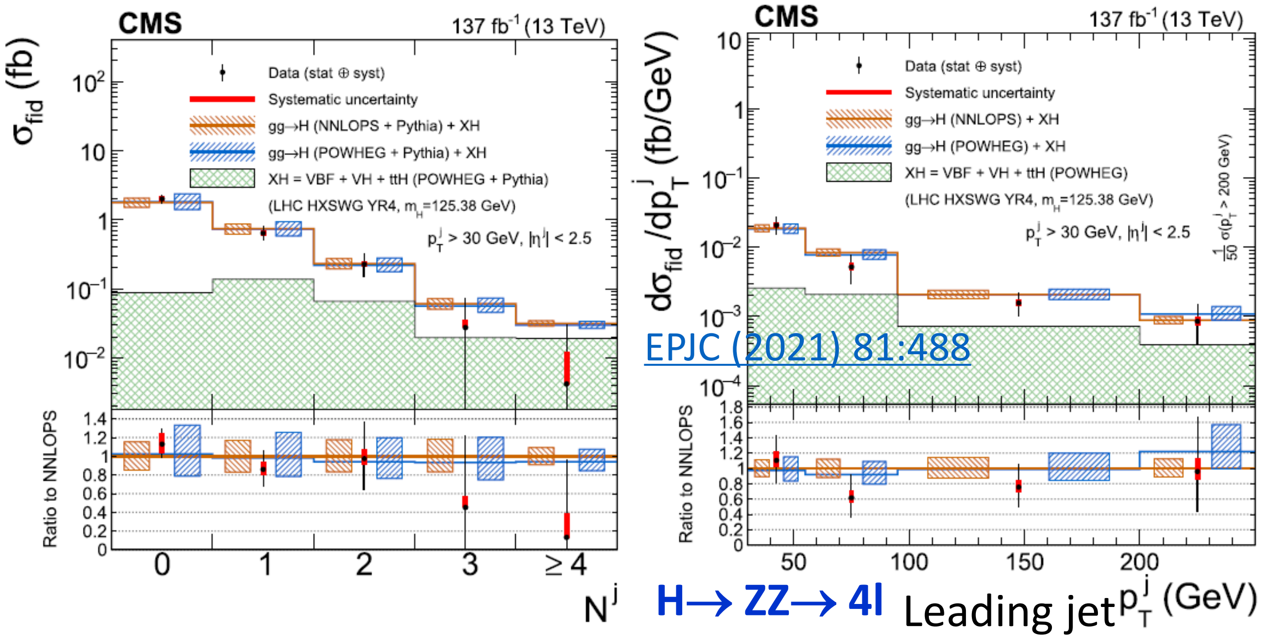

EPJC (2021) 81:488

H→ ZZ→ 4l

- **H→γγ**: For the **first time**, the cross section has been measured as a function of τ_C^j using up to six additional jets in the event, and $|\phi_\eta^*|$ for the diphoton system

$$\tau_C^j = \max_j \left(\frac{\sqrt{E_j^2 - p_{z,j}^2}}{2\cosh\left(Y_j - Y_H\right)} \right)$$

sensitive to Resummation (theory)

$$\phi_\eta^* = \tan\left(\frac{\phi_{acop}}{2}\right) \cdot \sin(\theta_\eta^*) \qquad \phi_{acop} = \pi - \Delta\phi$$

-- designed to probe **the low diphoton pT region** while minimizing the impact of experimental uncertainties

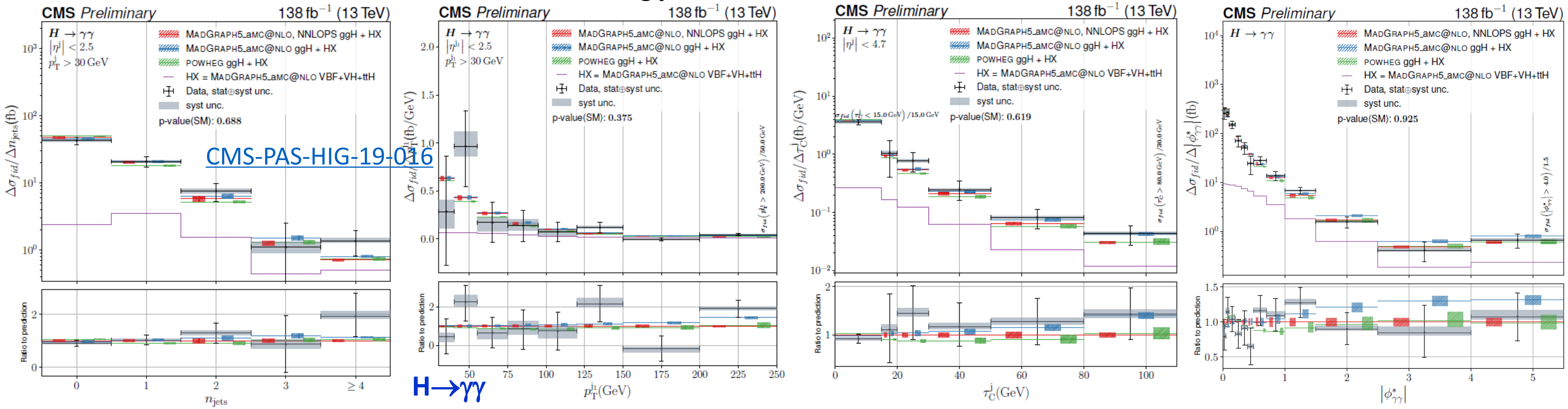

CMS-PAS-HIG-19-016

H→γγ

Double-differential fiducial cross section : H→γγ

➢ Two **double-differential cross section** measurements have been performed

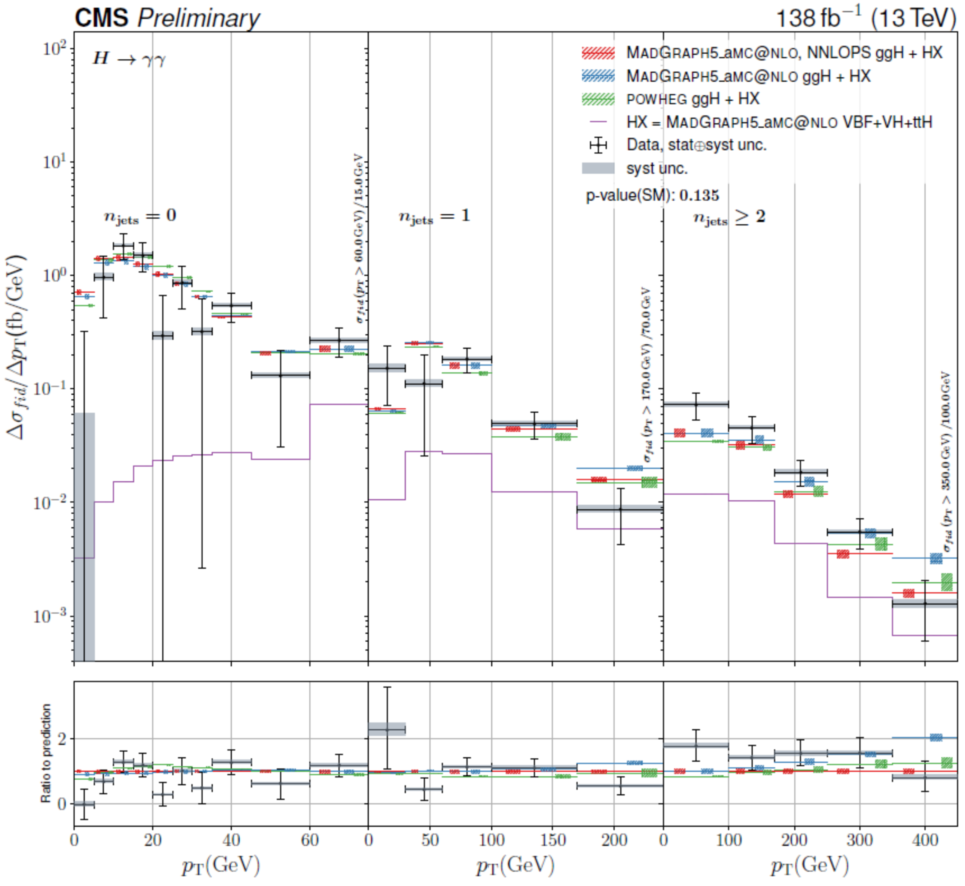

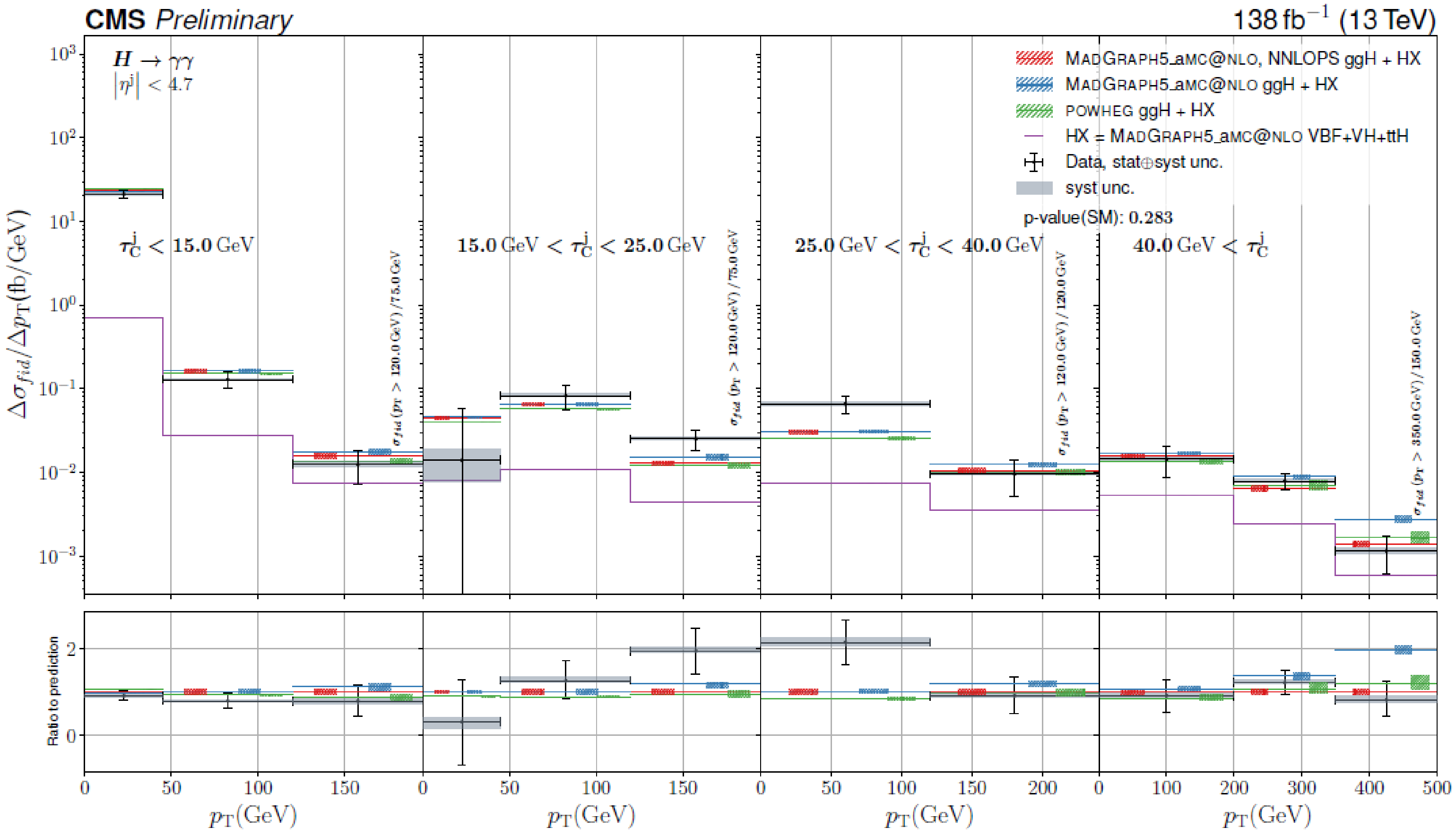

bins of $p_T^{\gamma\gamma}$ and n_{jets}

[CMS-PAS-HIG-19-016]

bins of $p_T^{\gamma\gamma}$ and τ_C^j

Higgs boson mass

- Importance of m_H in several aspects of our **understanding of fundamental physics**
  - ✓ **Precise higher order corrections to the theory predictions** of the Higgs interactions depend on the value of m_H
  - ✓ Input to **precision global fit** of the SM

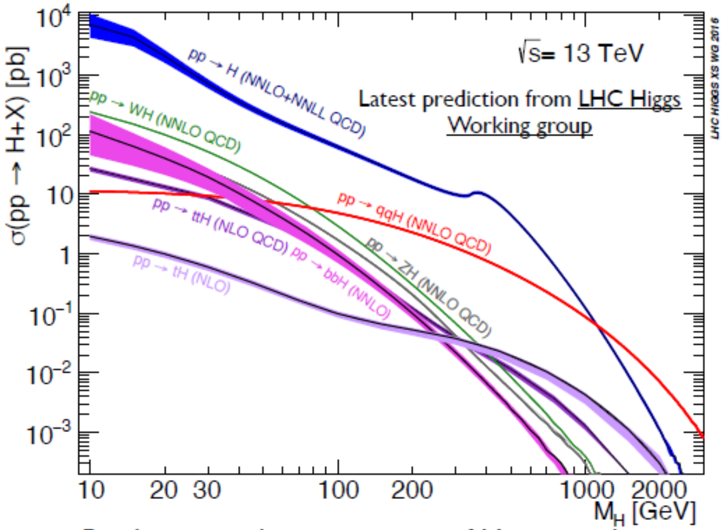

Prediction and uncertainties of Higgs production processes as a function of the m_H

Fundamental constants of the Standard Model

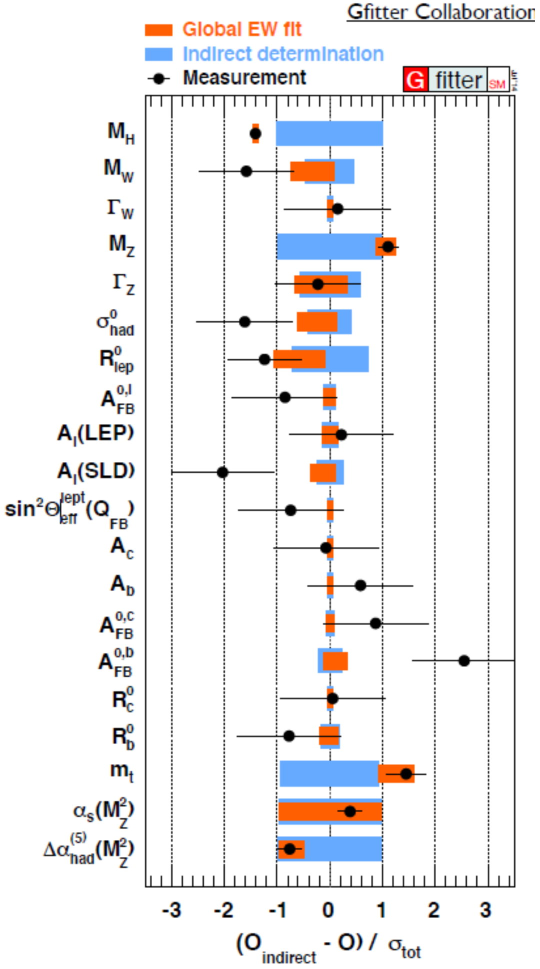

- **Free parameter** to be measured from the two high resolution channels: **H→ ZZ→** 4ℓ *and* **H→γγ**
  - ✓ ATLAS+CMS Run I precision on m_H of **2 per mille**
  - ✓ For both channels dominated by **statistical uncertainty** in Run1

PRL **114**, 191803

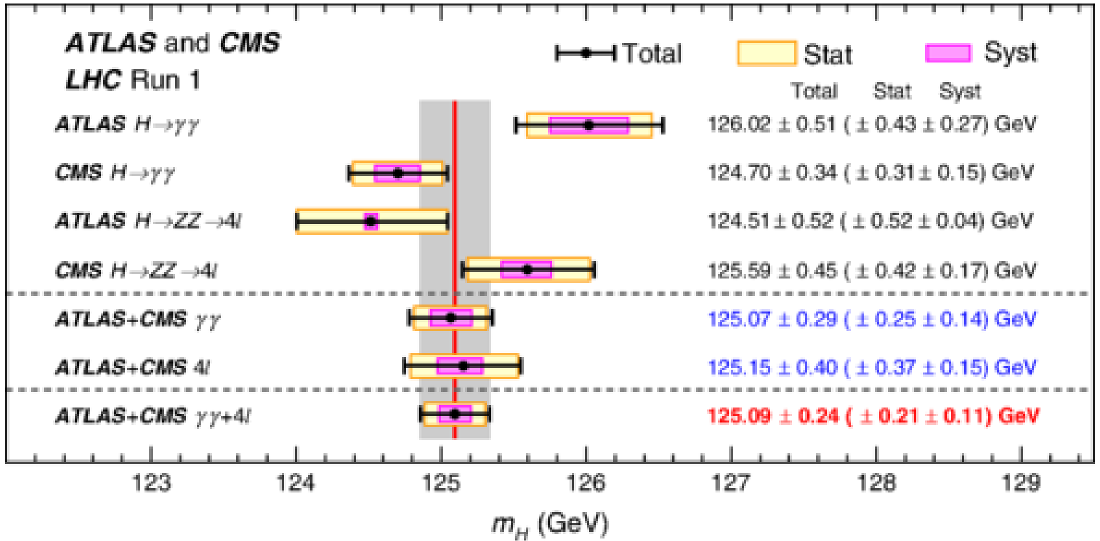

Higgs boson mass measurements

- Measured with **2016 legacy data :** analyses with full Run2 ultra-legacy data are still on going

- **H→ ZZ→ 4ℓ**
  - ✓ A mass constraint on the intermediate Z resonance Z_1
  - ✓ **Likelihood scan of 3D** of four-lepton mass, mass uncertainty and kinematic discriminant $\mathcal{L}(m'_{4\ell}, \mathcal{D}'_{\text{mass}}, \mathcal{D}^{\text{kin}}_{\text{bkg}})$

- **H→γγ**
  - ✓ events categorized into **3 VBF and 4 Untagged** (mainly ggH and all other events) categories
  - ✓ Special efforts made to **correct the energy scale more precisely** than before

    -- **Improved detector calibration** -> good agreement of the input variables to the energy regression correction

    -- **More precise** (granular Run-η-R9-pT dependent) **scale correction**

Source	Contribution (GeV)
Electron energy scale and resolution corrections	0.10
Residual p_T dependence of the photon energy scale	0.11
Modelling of the material budget	0.03
Nonuniformity of the light collection	0.11
Total systematic uncertainty	$\boxed{0.18}$
Statistical uncertainty	$\boxed{0.18}$
Total uncertainty	0.26

PLB 805 (2020) 135425

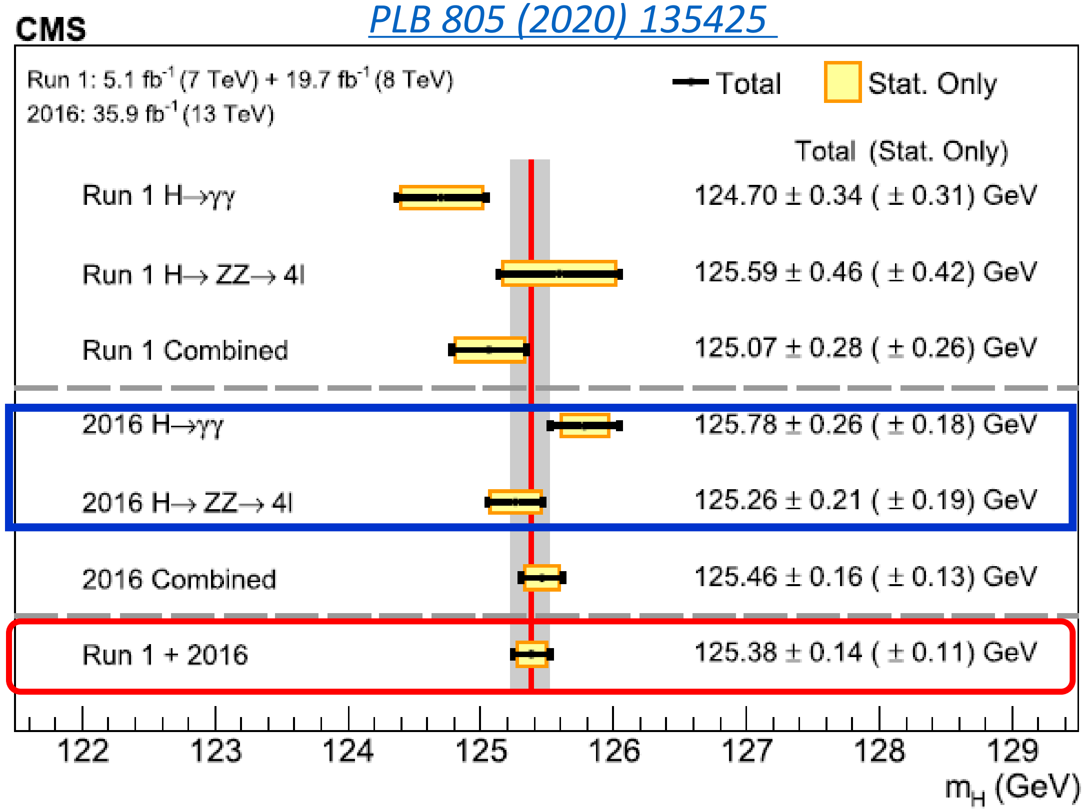

CMS 2016 precision: ~0.13%

CMS 2016 + Run1 precision: ~0.11%

Best precision to date (and more to come)

Stat. unc. dominant in 4ℓ channel

Stat. unc. comparable with the syst. unc. for γγ channel

Higgs boson mass projections at HL-LHC

- **Detector performance** such as acceptance, efficiency and resolution are considered to be **the same values as in Run2**
- Scale integrated luminosity to 3000 fb^{-1}
- **H→ ZZ→** 4ℓ
  - ✓ 9 categories based on the relative mass error
  - ✓ Z_1 mass constraint and beam spot constraint
  - ✓ 2D (four-lepton mas, kinematic discriminant) likelihood scan
  - ✓ Mass precision **~30 MeV**
- **H→γγ**
  - ✓ Projection based on 2016 results
  - ✓ Several **improvements** implemented in the **photon energy calibration** procedure : studied with ultra-legacy Run2 data
  - ✓ Mass precision **~70 MeV**

$m_{4\ell}$ expected uncertainty (MeV)	inclusive	4μ	4e	$2e2\mu$	$2\mu 2e$
Optimistic					
Total	26	30	105	60	67
Syst impact	16	11	64	31	32
Stat only	22	28	83	51	59
Pessimistic					
Total	30	32	206	107	112
Syst impact	20	15	189	94	95
Stat only	22	28	83	51	59

CMS-PAS-FTR-21-007

Sources of systematic uncertainty	Contribution [GeV]
Electron energy scale and resolution corrections	0.06
Residual p_T dependence of the photon energy scale	0.05
Modelling of the material budget	0.02
Statistical uncertainty	0.02
Total uncertainty	0.07

CMS-PAS-FTR-21-008

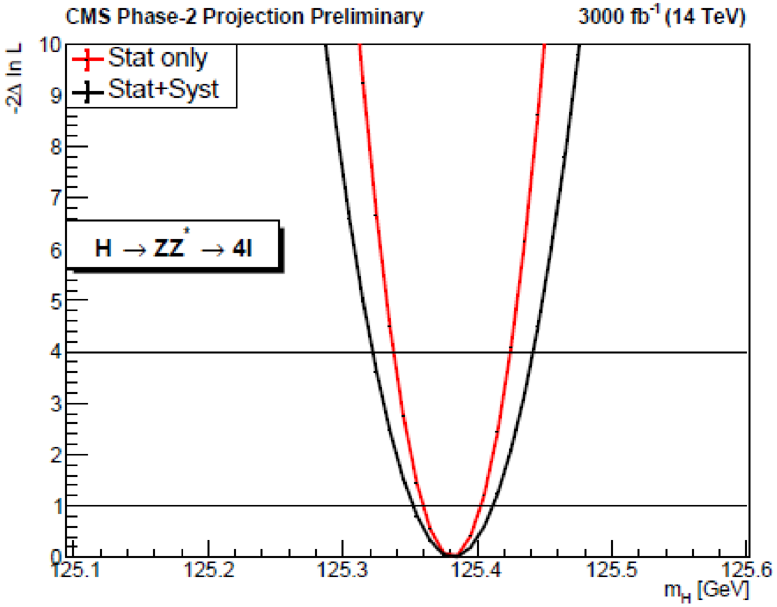

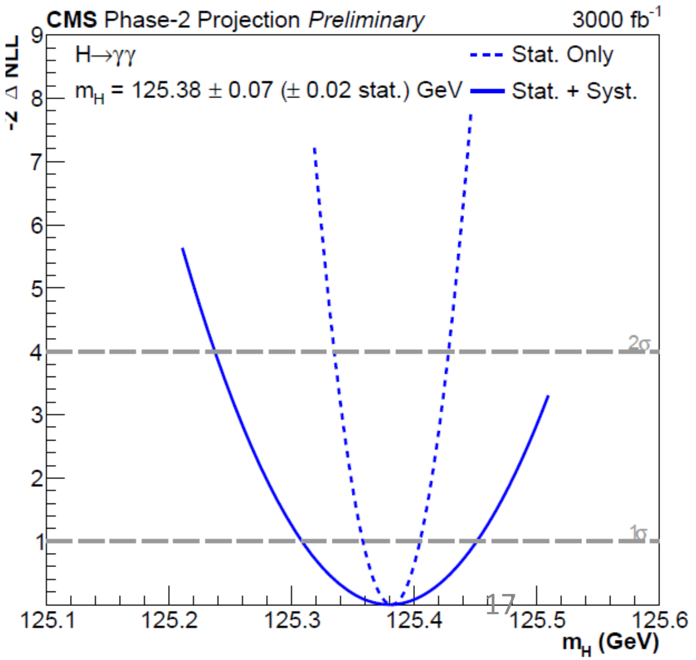

Summary

- H→ZZ→4ℓ and H→ $\gamma\gamma$ are two of the most important channels in the **measurements of Higgs boson properties**

- Higgs boson **cross sections** were measured with full Run2 data ~138 fb^{-1}
  - ✓ **Inclusive cross section precision is ~10% for each of 4ℓ and $\gamma\gamma$ channel**
  - ✓ **Fiducial cross sections were** measured in the dedicated phase regions
  - ✓ **Differential fiducial cross sections** as a function of the interesting observables related to Higgs boson production and decay, and **double differential observables** are measured
  - ✓ All measured results are **consistent**, within their uncertainties, with expectations of the Standard Model Higgs boson

- Higgs boson **mass** measurement have entered a precise era at LHC
  - ✓ **Current most precise $\boldsymbol{m_H}$ measurement** ~0.11% with **2016 data (36 fb^{-1})**
  - ✓ Full Run2 measurements still ongoing … stay tune!
  - ✓ HL-LHC is expected to bring a more precise results : ~0.02%

- **Run3 results … stay tune!**

Thanks for your attention!

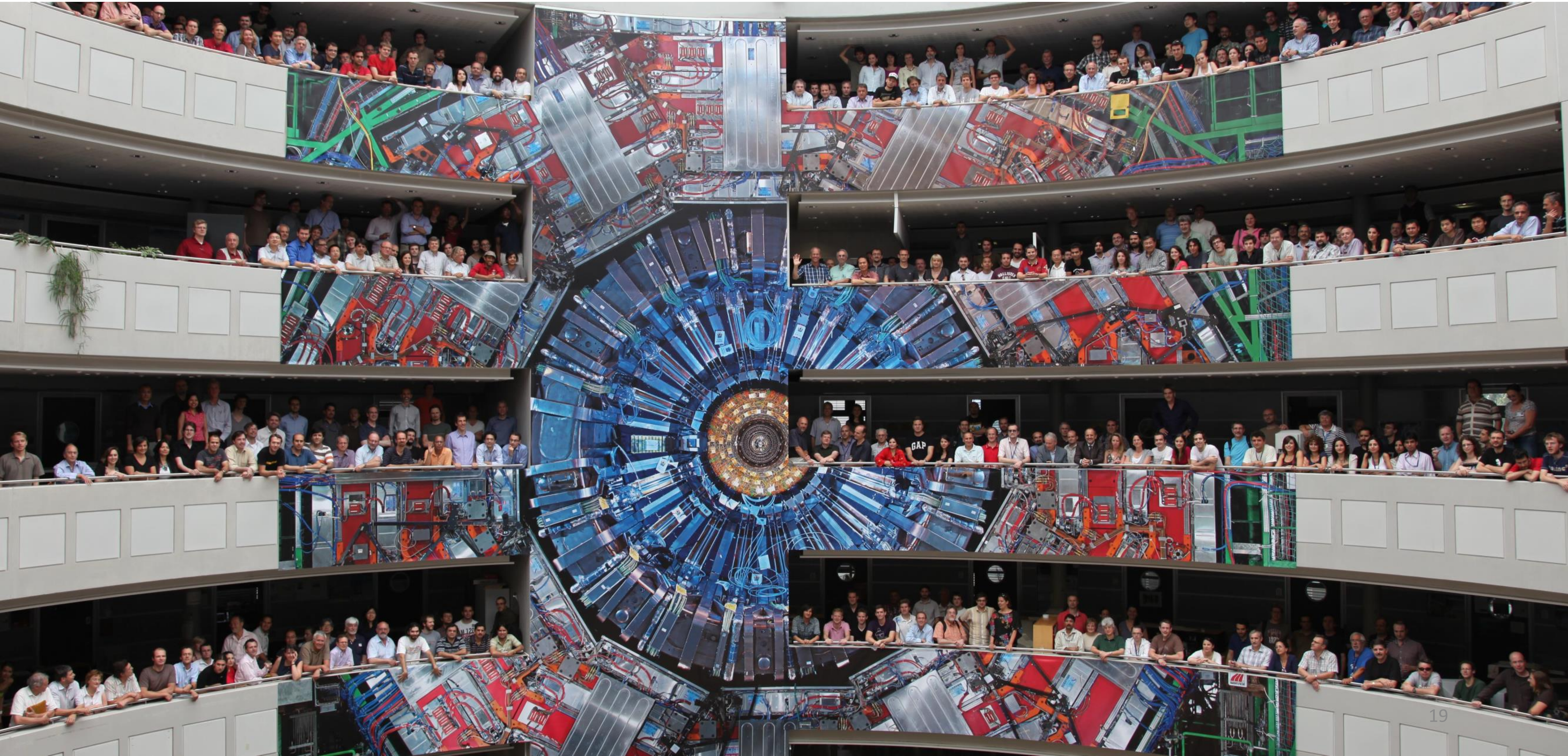

Backup

Higgs production

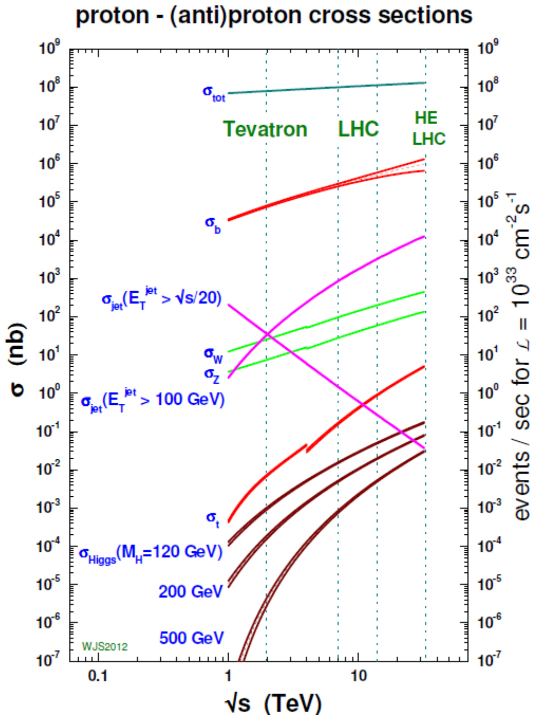

- Production rates of Higgs many orders smaller than of background processes
- Trigger, analysis selections, and background estimation needs careful design

Higgs bosons per fb^{-1} (13 TeV)

	produced	selected
$H \to \gamma\gamma$	130	46
$H \to ZZ^*$	1400	1.5
$H \to WW^*$	12000	42
$H \to \tau\tau$	3500	17
$H \to b\bar{b}$	32000	66

Also due to $Z \to \ell\ell$ and $W \to \ell\nu$ BFs

Phys. Rev. D 101 (2020) 012002

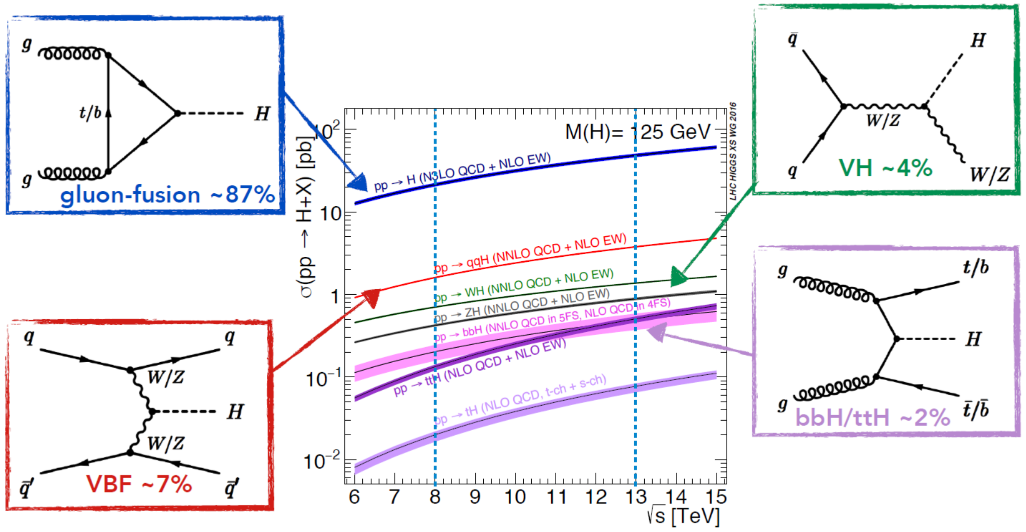

- **Significant increase in production cross section from 8 TeV (Run1 2012) to 13 TeV (Run2)**
  - ✓ $\sigma_{13TeV}/\sigma_{8TeV}$ of Higgs: ggH ~2.3, VBF ~2.4, VH ~2.0 and **ttH ~3.9**
  - ✓ *background increased by a factor of ~2*

ECAL response changes over Run 1 and Run 2

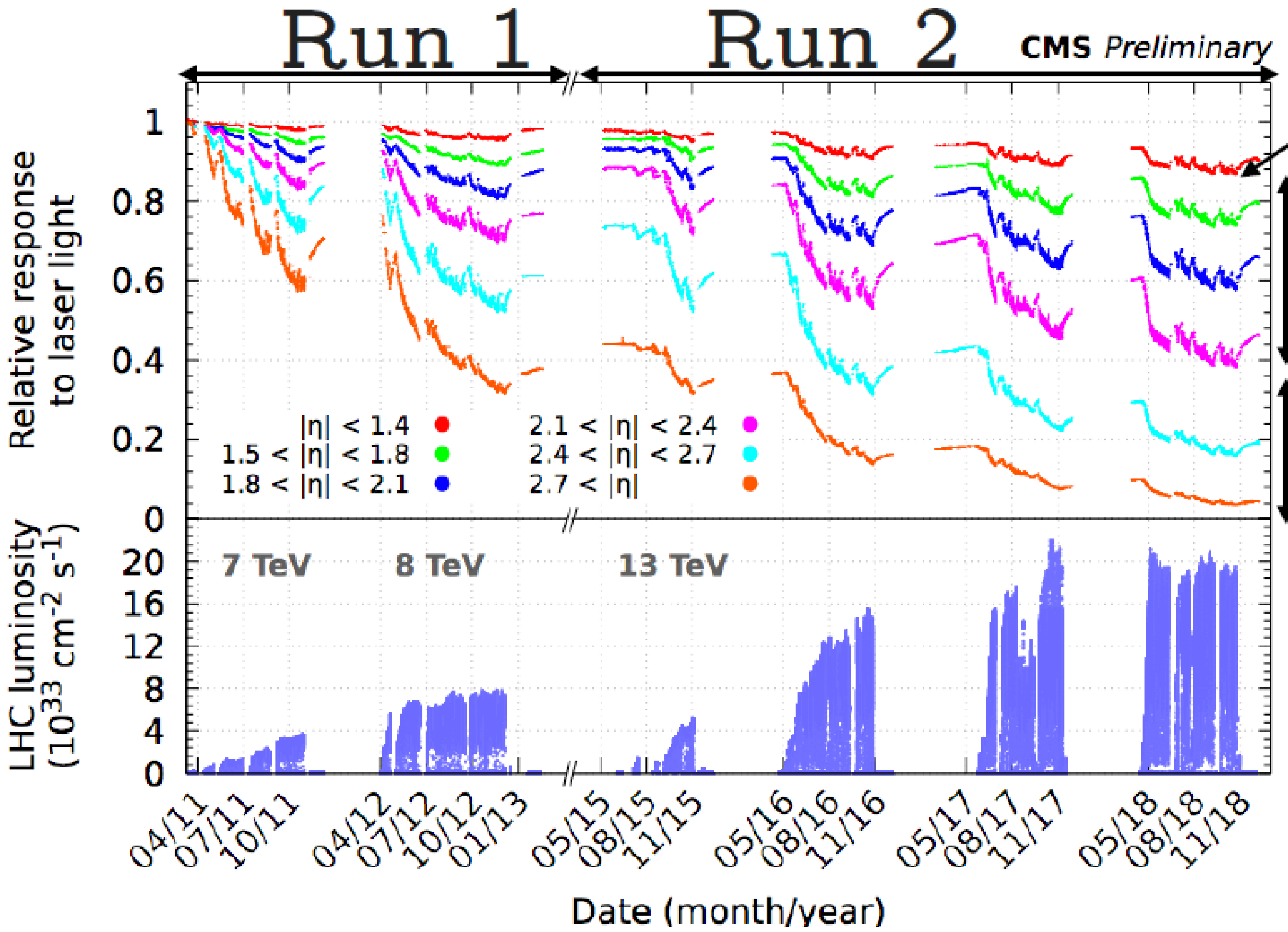

Barrel (13%)

Endcap region covered by CMS tracker (62%)

Endcap region relevant for forward jets: low response (max: 96% loss) due to ageing induces amplification of the noise: Noise mitigation is performed with optimized energy clustering

Significant response changes (crystal+photodetector) due to LHC irradiation
Monitoring of each channel via a dedicated laser system, is performed every 40 minutes and corrections are provided within 48 hours.
These are crucial to **maintain stable ECAL energy scale and resolution** over time

Some detailed Analysis strategy of H→γγ

Analysis flow

- Data & MC
- Trigger
- Photon reconstruction and energy calibration
- Preselection
- Vertex identification and probability estimation
- Photon identification
- Diphoton BDT
- Selections of event categories : exclusive-/untagged
- Signal/bkg modeling
- Statistical analysis with "combine"
- **Results**

Photon Energy scale and resolution validated with Z→ee

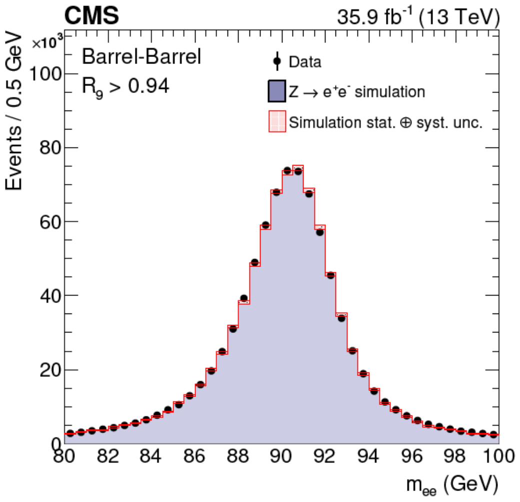

BDT for vertex identification : validated on Z→μμ and γ+j

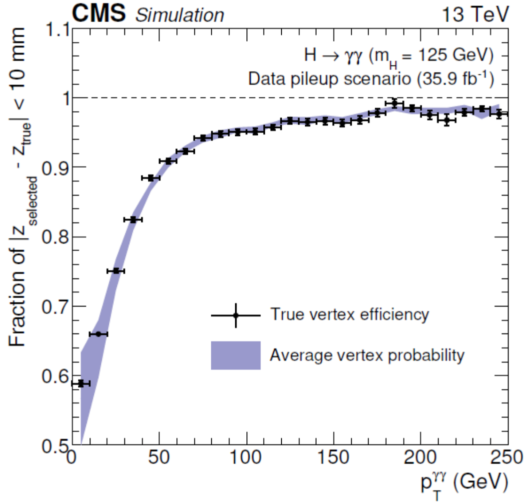

[JHEP 11 (2018) 185]

Photon ID BDT to discriminate prompt/fake photons

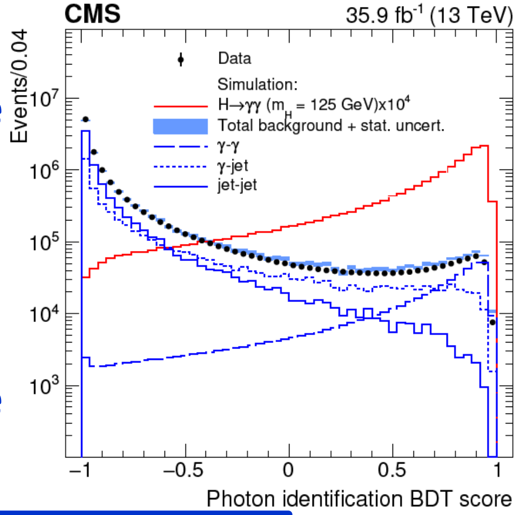

Diphoton BDT to discriminate signal and bkg

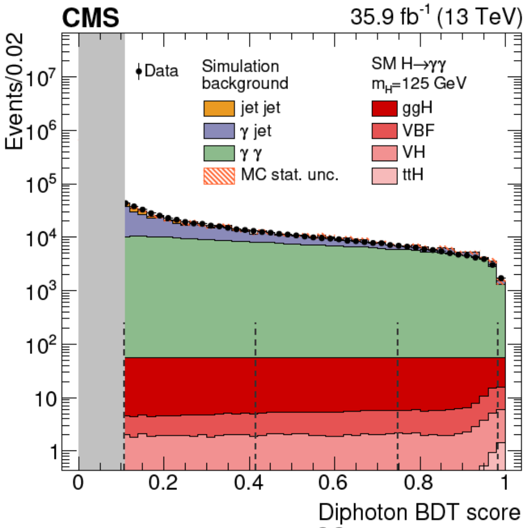

Common tools for different H→γγ measurements

$m_{\gamma\gamma}$: primary vertex identification

$$m_{\gamma\gamma} = \sqrt{2E_1E_2(1-\cos\theta)}$$

➢ Vertex assignment correct within **1 cm → has negligible** impact on mass resolution

➢ **Multivariate approach (BDT) for vertex identification**

- Vertex ID BDT: **kinematic correlations and track distribution imbalance**

$$\sum_i |\vec{p}_T^{\,i}|^2 \,,\, -\sum_i \left(\vec{p}_T^{\,i} \cdot \frac{\vec{p}_T^{\,\gamma\gamma}}{|\vec{p}_T^{\,\gamma\gamma}|}\right) \text{ and } \left(|\sum_i \vec{p}_T^{\,i}| - p_T^{\gamma\gamma}\right) / \left(|\sum_i \vec{p}_T^{\,i}| + p_T^{\gamma\gamma}\right)$$

- if conversions are present **conversion information**
  - the number of conversions,
  - the pull $|z_{\mathrm{vtx}} - z_{\mathrm{e}}|/\sigma_z$ between the longitudinal position of the reconstructed vertex, z_{vtx}, and the longitudinal position of the vertex estimated using conversion track(s), z_{e}, where the variable σ_z denotes the uncertainty on z_{e}.

➢ A second MVA estimates **probability of correct vertex** choice, used for di-photon classification using BDT

➢ **Method validated** on Z→μμ events where vertex found after removing muon tracks and γ+j for converted γ

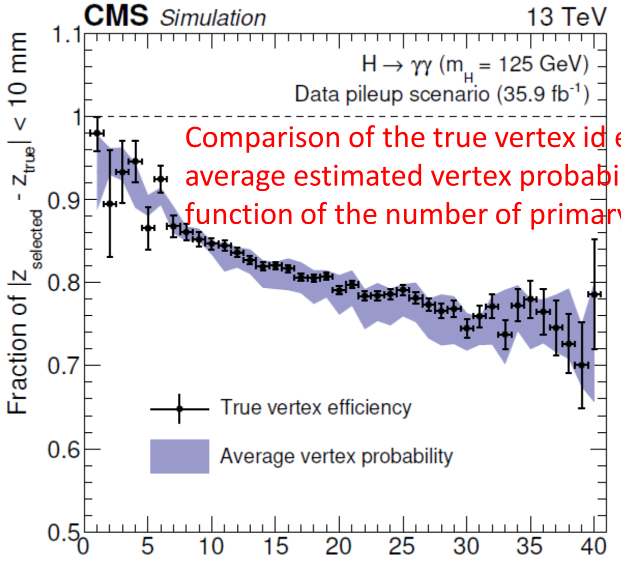

Averaged efficiency is about 81%

JHEP 11 (2018) 185

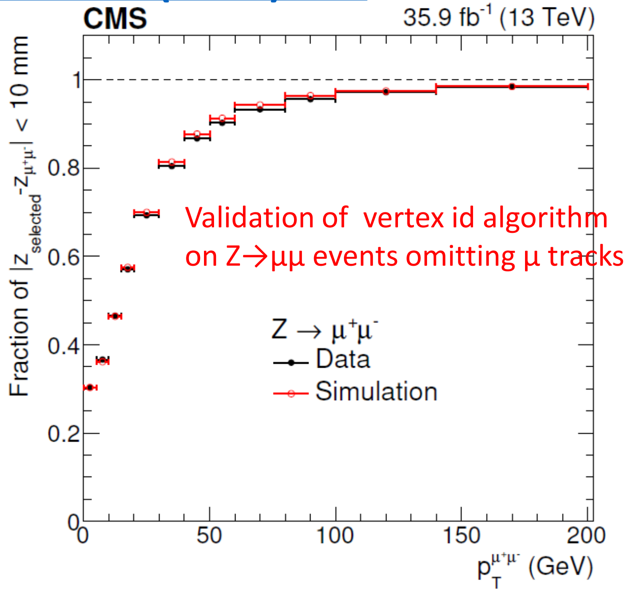

Impact of the main sources of systematic uncertainty

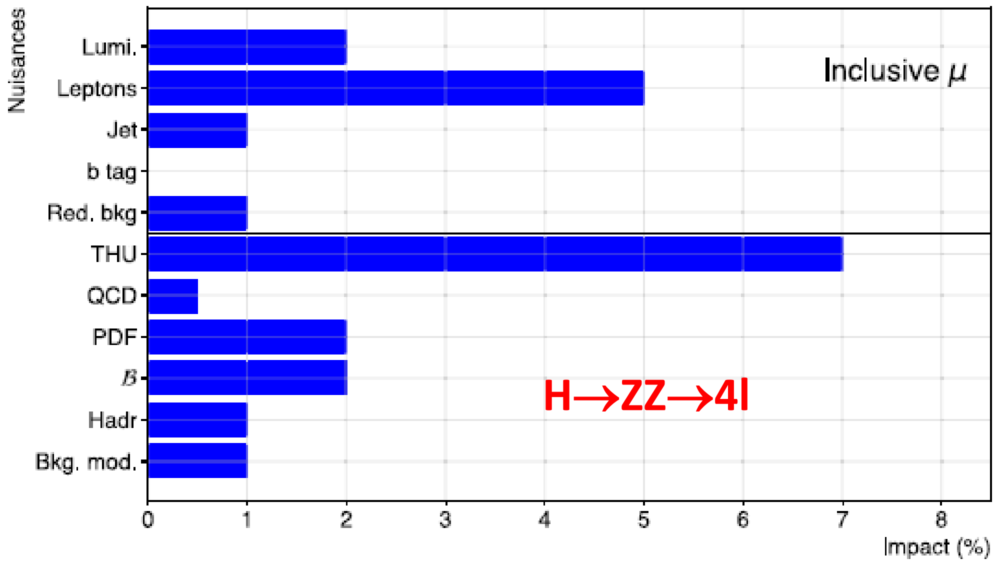

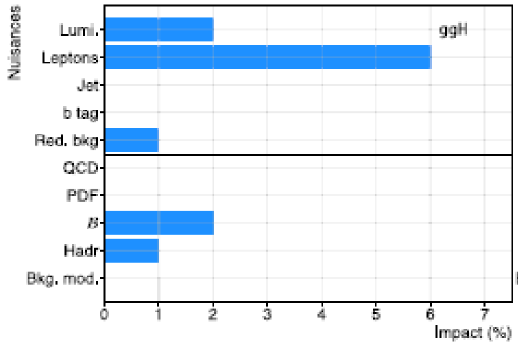

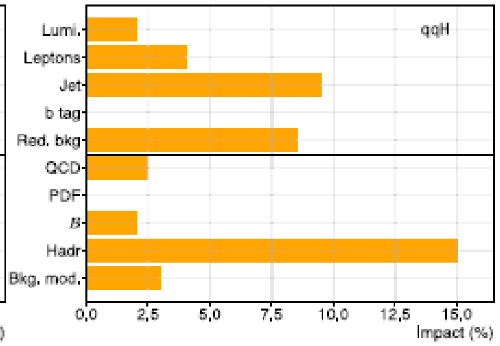

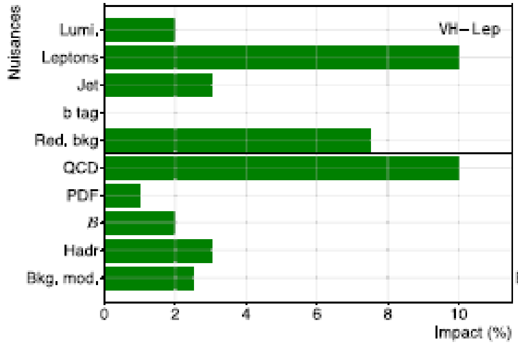

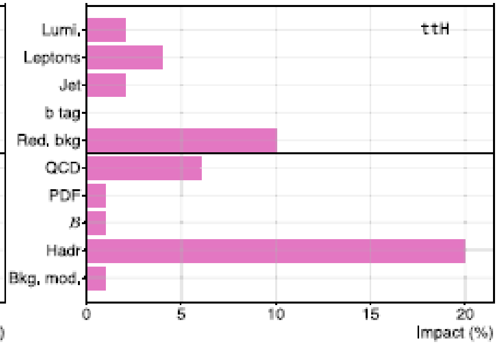

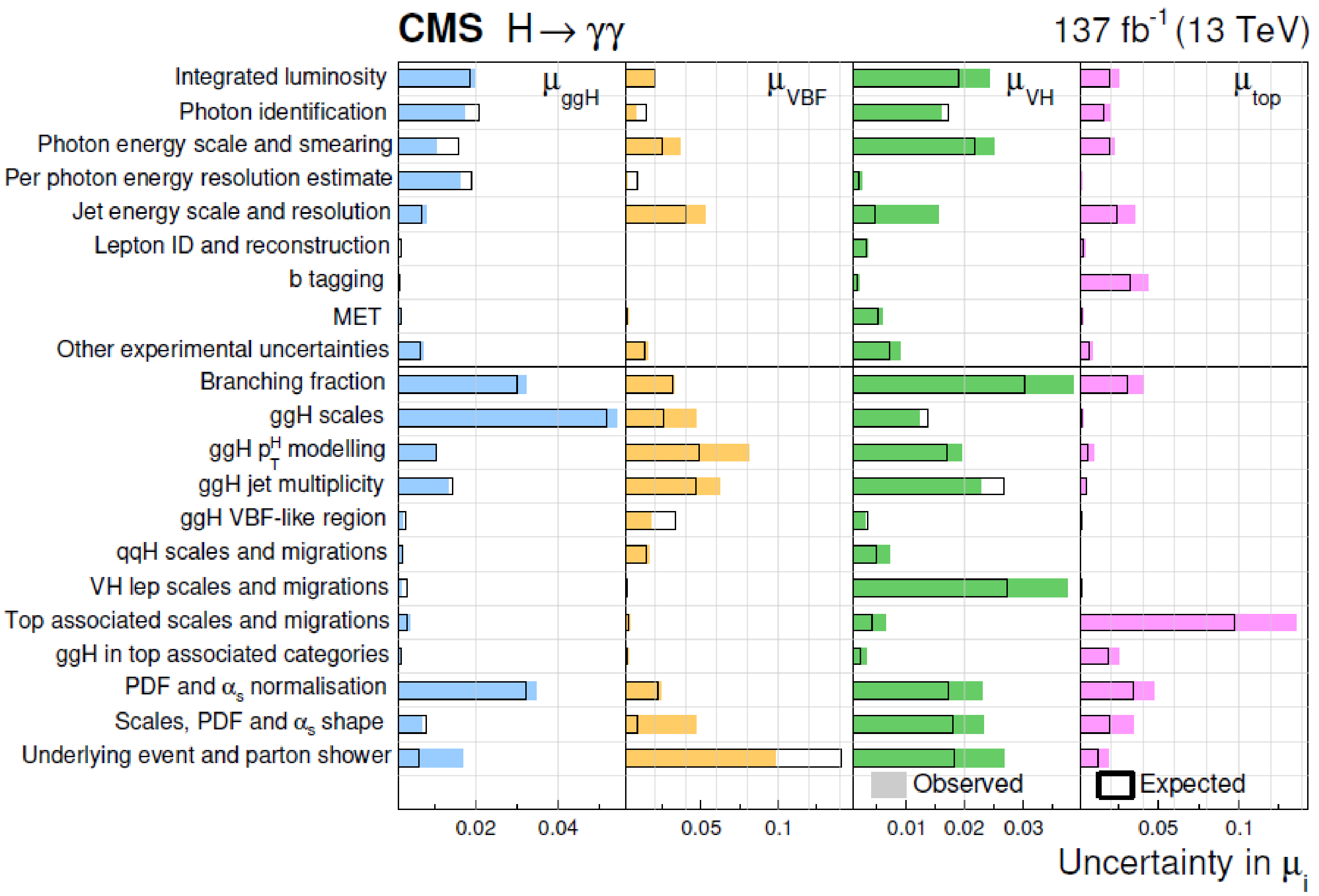

Signal strengths, cross sections

Nature 607 (2022) 60
Nature 607 (2022) 52

- A global signal strength scaling all channels:

$$\mu = 1.002 \pm 0.057 = 1.002 \pm 0.036\,(\text{theo}) \;\pm 0.033\,(\text{syst}) \;\pm 0.029\,(\text{stat}) \quad \textbf{CMS}$$

$$\mu = 1.05 \pm 0.06 = 1.05 \pm 0.04\,(\text{theo}) \;\pm 0.03\,(\text{syst}) \;\pm 0.03\,(\text{stat}) \quad \textbf{ATLAS}$$

- Improvement in relative precision: 14% (Run 1) ➔ **6%** (Run 2)
  - Theory uncertainty: 7% (Run 1) ➔ 4% (Run 2)

Combined measurements: ingredients

- Individual analyses study **specific** Higgs boson characteristics
  ➔ need to **combine** them to get a **full view** of the Higgs boson
- Targeted signatures **included in combined measurements**:

	ggH	qqH	VH	ttH/tH
H→γγ	ATLAS CMS	ATLAS CMS	ATLAS CMS	ATLAS CMS
H→ZZ	ATLAS CMS	ATLAS CMS	ATLAS CMS	ATLAS CMS
H→WW	ATLAS CMS	ATLAS CMS	ATLAS CMS	ATLAS CMS
H→ττ	ATLAS CMS	ATLAS CMS	ATLAS CMS	ATLAS CMS
H→bb	ATLAS CMS	ATLAS	ATLAS CMS	ATLAS CMS
H→μμ	ATLAS CMS	ATLAS CMS	ATLAS CMS	ATLAS CMS
H→cc			ATLAS	
H→Zγ	ATLAS CMS	ATLAS CMS	ATLAS CMS	ATLAS CMS
H→inv	CMS	ATLAS CMS	ATLAS CMS	

Most of the main production x decay channels included

Note: some additional channels not yet included in combined measurements

Rare decay modes starting to feature in combined measurements

Searches for invisible H decays (for coupling strengths)

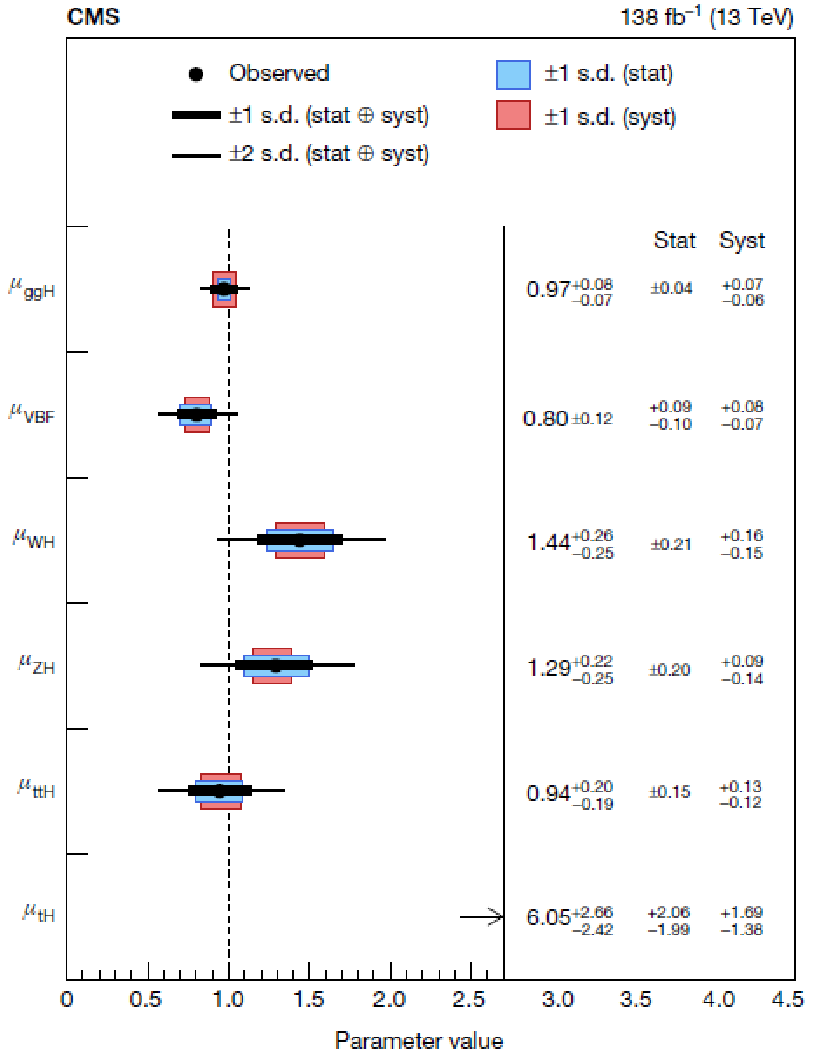

H→ZZ→4ℓ STXS bins

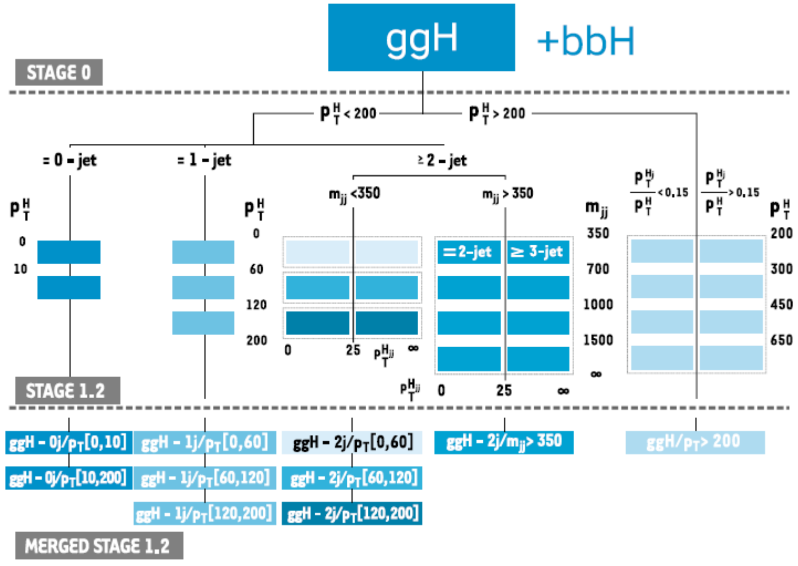

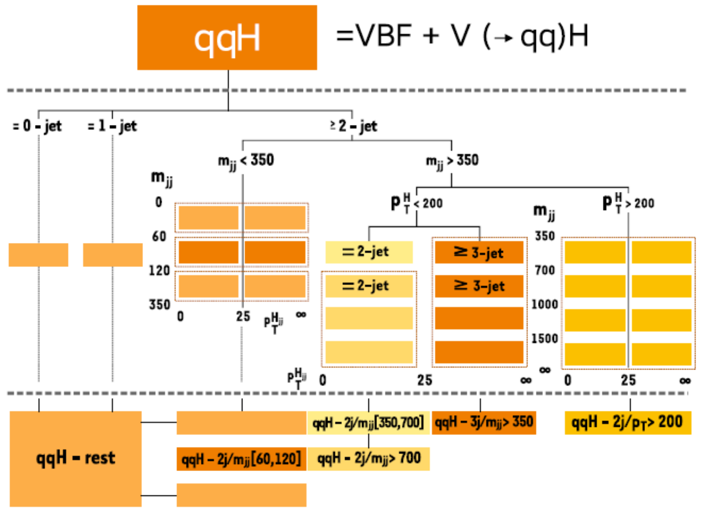

EPJC (2021) 81:488

STXS stage 1.2 bins used in H→ZZ→4l analysis

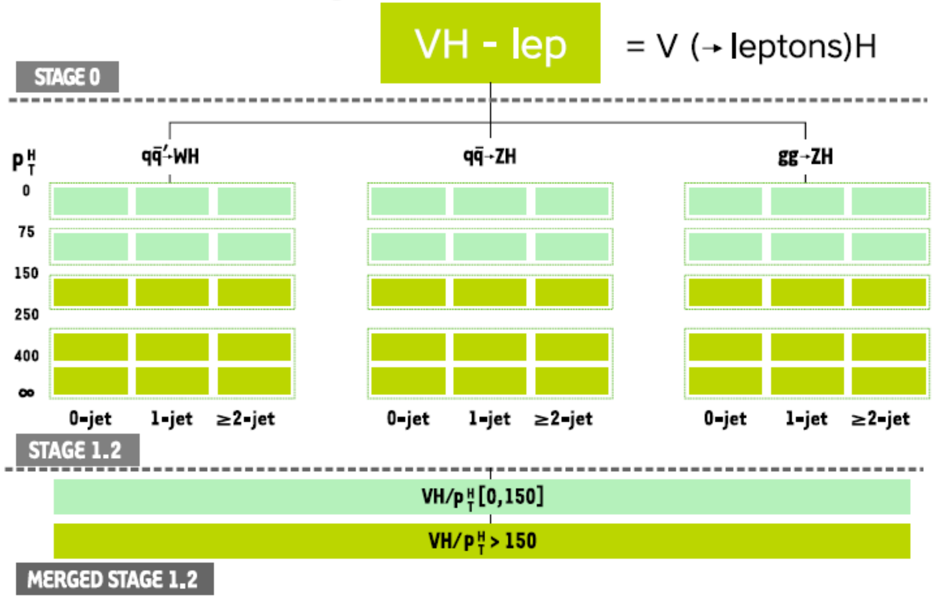

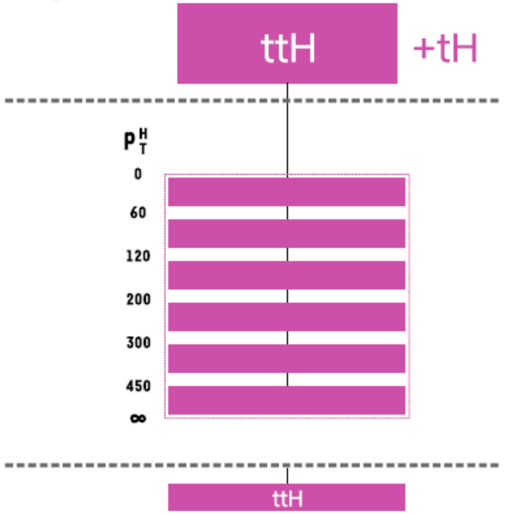

Correlation matrices

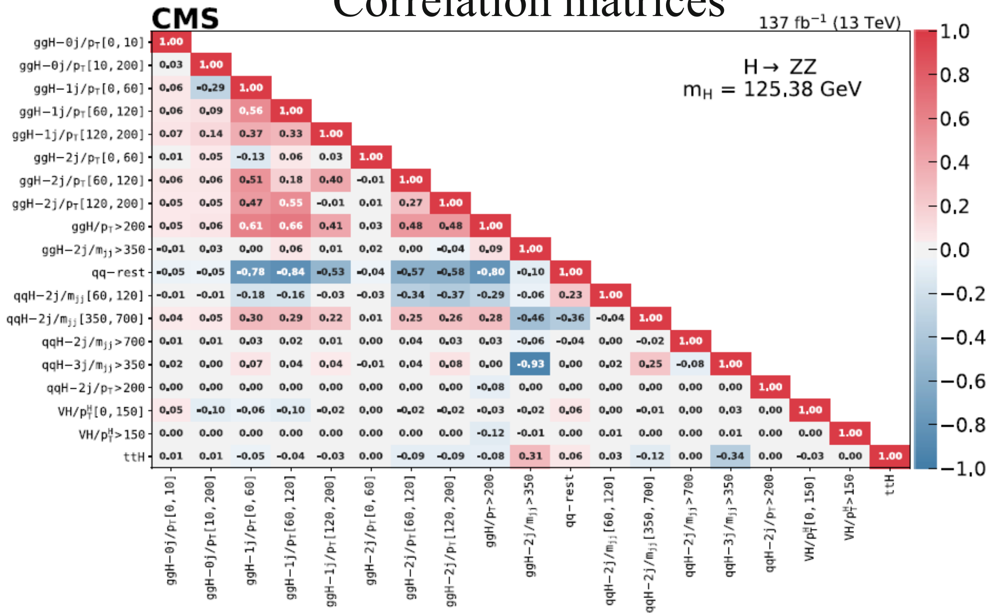

The composition of the analysis categories in terms of a merged set of STXS bins is shown.

The colour scale corresponds to the fractional yield in each analysis category group (rows) accounted for by each STXS process (columns)

Each row therefore sums to 100%. Entries with values less than 0.5% are not shown

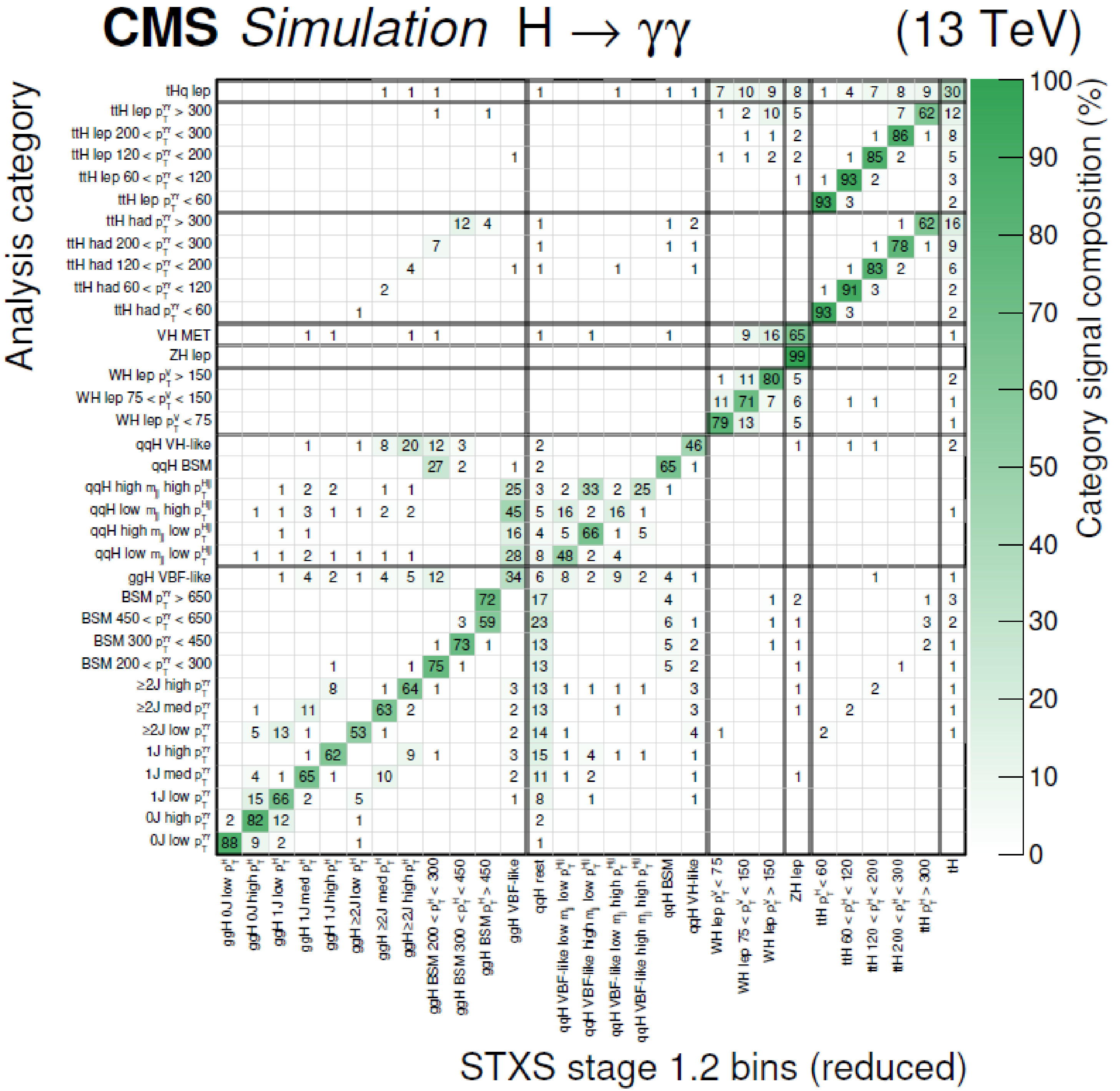

H→γγ STXS bin correlations

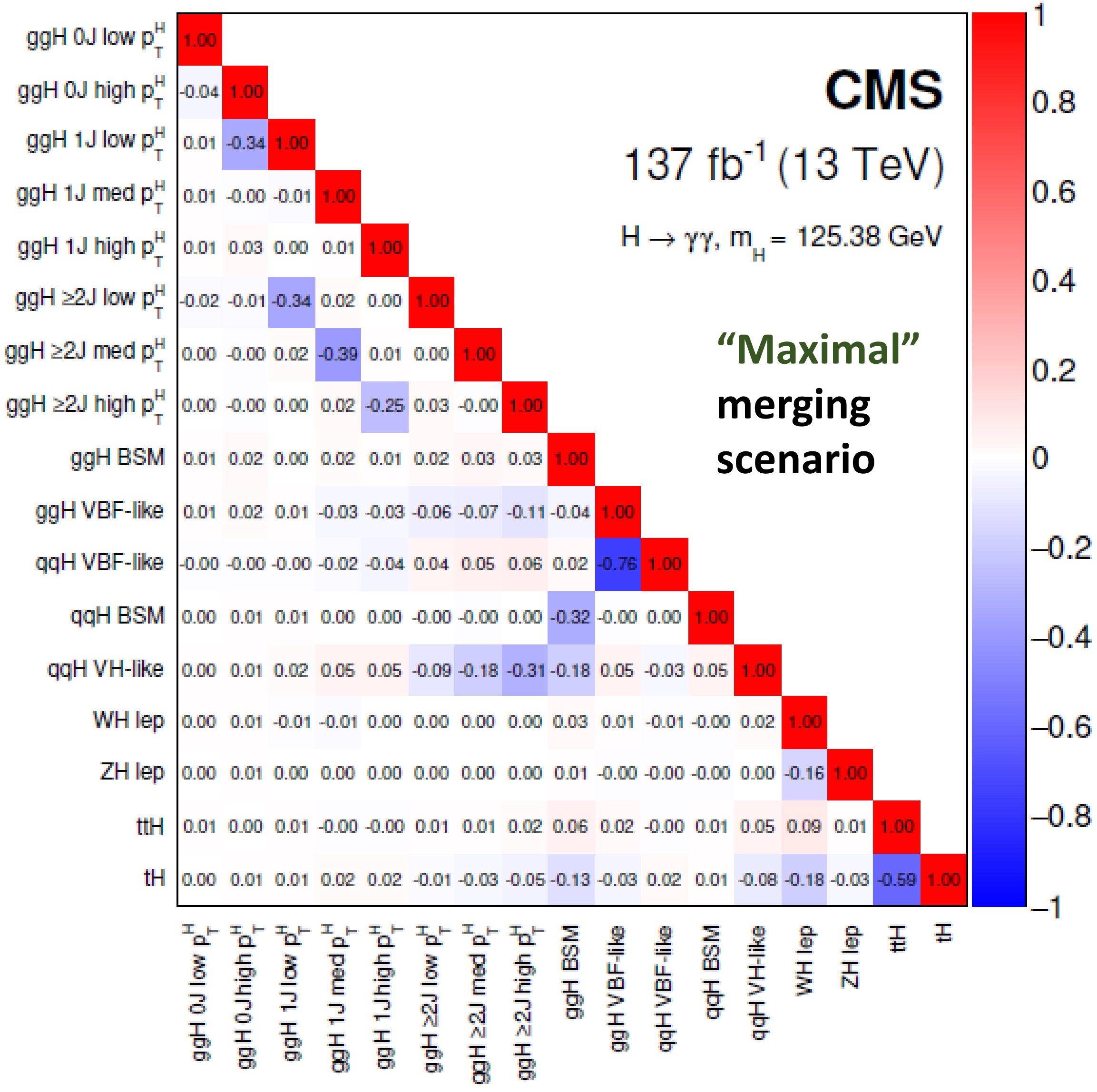

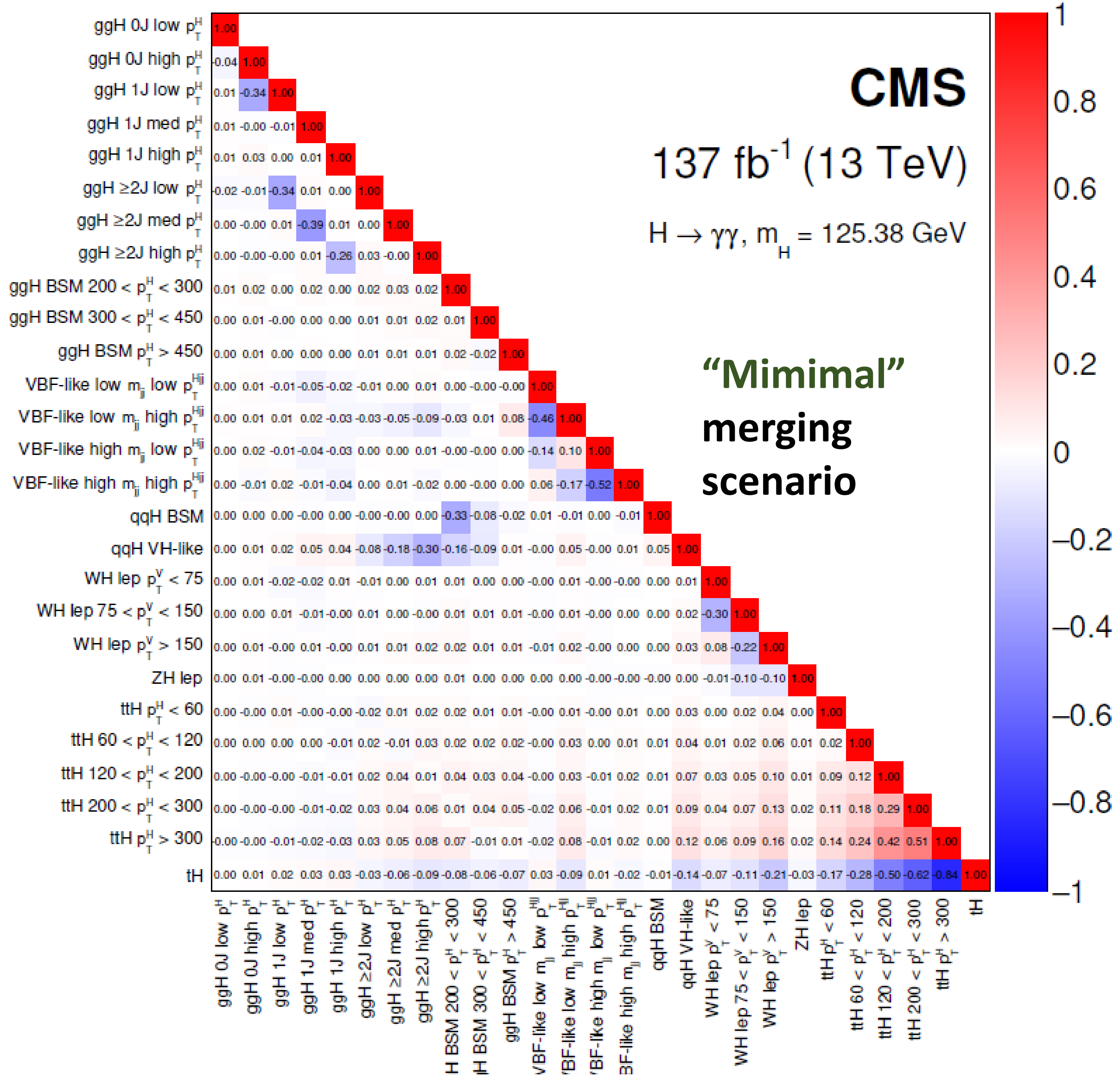

Binning for 4l (left two) VS $\gamma\gamma$ (right) of 1D differential xsec

EPJC (2021) 81:488

Table 10 The measured differential fiducial cross section and ±1 standard deviation uncertainties for the p_T^H observable at m_H = 125.38 GeV. The breakdown of the total uncertainty (unc.) into statistical and systematic components is given

Bin range (GeV)	$d\sigma_{fid}$ (fb)	unc.	(stat)	(syst)
0–10	0.32	$^{+0.11}_{-0.10}$	$^{+0.10}_{-0.09}$	$^{+0.04}_{-0.03}$
10–20	0.67	$^{+0.14}_{-0.13}$	$^{+0.13}_{-0.12}$	$^{+0.06}_{-0.05}$
20–30	0.41	$^{+0.12}_{-0.10}$	$^{+0.11}_{-0.10}$	$^{+0.04}_{-0.04}$
30–45	0.51	$^{+0.12}_{-0.10}$	$^{+0.11}_{-0.10}$	$^{+0.04}_{-0.04}$
45–80	0.45	$^{+0.10}_{-0.09}$	$^{+0.10}_{-0.09}$	$^{+0.04}_{-0.03}$
80–120	0.30	$^{+0.08}_{-0.07}$	$^{+0.07}_{-0.07}$	$^{+0.02}_{-0.02}$
120–200	0.19	$^{+0.06}_{-0.05}$	$^{+0.06}_{-0.05}$	$^{+0.01}_{-0.01}$
200–13000	0.03	$^{+0.02}_{-0.02}$	$^{+0.02}_{-0.01}$	$^{+0.00}_{-0.00}$

Table 11 The measured differential fiducial cross section and ±1 standard deviation uncertainties for the $|y^H|$ observable at m_H = 125.38 GeV. The breakdown of the total uncertainty (unc.) into statistical and systematic components is given

Bin range	$d\sigma_{fid}$ (fb)	unc.	(stat)	(syst)
0.0–0.15	0.41	$^{+0.10}_{-0.08}$	$^{+0.09}_{-0.08}$	$^{+0.05}_{-0.03}$
0.15–0.3	0.36	$^{+0.08}_{-0.07}$	$^{+0.07}_{-0.07}$	$^{+0.03}_{-0.02}$
0.3–0.6	0.62	$^{+0.13}_{-0.11}$	$^{+0.11}_{-0.10}$	$^{+0.07}_{-0.05}$
0.6–0.9	0.57	$^{+0.12}_{-0.10}$	$^{+0.10}_{-0.10}$	$^{+0.06}_{-0.04}$
0.9–1.2	0.36	$^{+0.10}_{-0.09}$	$^{+0.09}_{-0.08}$	$^{+0.05}_{-0.03}$
1.2–2.5	0.64	$^{+0.15}_{-0.13}$	$^{+0.13}_{-0.12}$	$^{+0.08}_{-0.05}$

H→ ZZ→ 4l

HIG-21-009

Variable	Binning
$p_T(H)$	[0.0, 10, 20, 30, 45, 60, 80, 120, 200, ∞]
$\|y(H)\|$	[0.0, 0.15, 0.3, 0.45, 0.6, 0.75, 0.9, 1.2, 1.6, 2.5]
m_{Z1}	[40,65,73,80,85,90,120]
m_{Z2}	[12,22,25,28,30,32,35,40,50,65]
$\cos\theta^*$	[-1.0, -0.75, -0.5, -0.25, 0.0, 0.25, 0.5, 0.75, 1.0]
$\cos\theta_1$	[-1.0, -0.75, -0.5, -0.25, 0.0, 0.25, 0.5, 0.75, 1.0]
$\cos\theta_2$	[-1.0, -0.75, -0.5, -0.25, 0.0, 0.25, 0.5, 0.75, 1.0]
Φ	$[-\pi, -3/4\pi, -\pi/2, -\pi/4, 0, \pi/4, \pi/2, 3/4\pi, \pi$
Φ_1	$[-\pi, -3/4\pi, -\pi/2, -\pi/4, 0, \pi/4, \pi/2, 3/4\pi, \pi$
p_T^{j1}	[0-jet, 30, 55, 95, 200, ∞]
p_T^{j2}	[0/1-jet, 30, 40, 65, 90, ∞]
m_{4l}^j	[0-Jet, 110, 180, 220, 300, 400, 600, ∞]
m_{jj}	[0/1-jet, 0, 120, 300, ∞]
$\|\Delta\eta_{jj}\|$	[0/1-jet, 0.0, 0.7, 1.6, 3, ∞]
$\Delta\phi_{jj}$	$[0/1\text{-jet}, -\pi, -\pi/2, 0, \pi/2, \pi]$
p_T^{Hjj}	[0/1-jet, 0,20,60,110,∞]
τ_C^{jmax}	$[0\text{-jet}(\tau_C^{jmax} < 15), 15, 20, 30, 50, 80, \infty]$
τ_B^{jmax}	$[0\text{-jet}(\tau_B^{jmax} < 30), 30, 70, 130, 250, 400, \infty]$
D_0^-	[0.0, 0.4, 0.5, 0.6, 0.7, 0.8, 0.9, 1.0]
D_{CP}	[-0.75, -0.25, -0.1, 0.0, 0.1, 0.25, 0.75]
D_0^{hp}	[0.0, 0.35, 0.4, 0.45, 0.55, 0.65, 0.75, 1]
D^{int}	[0.0, 0.7, 0.8, 0.9, 0.95, 1.0]
D_{L1}	[0.0, 0.45, 0.5, 0.6, 0.7, 1.0]
$D_{L1}^{Z\gamma}$	[0.0, 0.35, 0.45, 0.5, 0.55, 0.65, 1.0]

Table 3: Binning per observable of interest. The first row of the table shows the observables measured in the baseline fiducial phase space, the second one observables involving one extra jet, and the third one involving two or more extra jets. In the fourth row observables for the VBF-enriched phase space are shown.

H→$\gamma\gamma$

CMS-PAS-HIG-19-016

Phase Space Region	Observable	Bin boundaries							
Baseline $p_T^{\gamma_1}/m_{\gamma\gamma} > 1/3$ $p_T^{\gamma_2}/m_{\gamma\gamma} > 1/4$ $\|\eta^\gamma\| < 2.5$ $\mathcal{I}_{gen}^\gamma < 10\,GeV$	$p_T^{\gamma\gamma}$	0	5	10	15	20	25	30	35
		45	60	80	100	120	140	170	200
		250	350	450	∞				
	n_{jets}	0	1	2	3	≥ 4			
	$\|y^{\gamma\gamma}\|$	0.0	0.1	0.2	0.3	0.45	0.6	0.75	0.90
		2.5							
	$\|\cos(\theta^*)\|$	0.0	0.07	0.15	0.22	0.35	0.45	0.55	0.75
		1.0							
	$\|\phi_\eta^*\|$	0.0	0.05	0.1	0.2	0.3	0.4	0.5	0.7
		1.0	1.5						
		2.5	4.0	∞					
	$p_T^{\gamma\gamma}, n_{jets} = 0$	0	5	10	15	20	25	30	35
		45	60	∞					
	$p_T^{\gamma\gamma}, n_{jets} = 1$	0	30	60	100	170	∞		
	$p_T^{\gamma\gamma}, n_{jets} > 1$	0	100	170	250	350	∞		
	n_{jets}^b	0	1	≥ 2					
	$n_{leptons}$	0	1	≥ 2					
	p_T^{miss}	0	30	50	100	200	∞		
1-jet Baseline + ≥ 1 jet $p_T^j > 30$ GeV $\|\eta^j\| < 2.5$	$p_T^{j_1}$	30	40	55	75	95	120	150	200
		∞							
	$\|y^{j_1}\|$	0.0	0.3	0.6	0.9	1.2	1.6	2.0	2.5
	$\|\Delta\phi_{\gamma\gamma,j_1}\|$	0.0	2.0	2.6	2.85	3.0	3.07	π	
	$\|\Delta y_{\gamma\gamma,j_1}\|$	0.0	0.3	0.6	1.0	1.4	1.9	2.5	∞
	τ_C^j	< 15	15	20	30	50	80	∞	
	$p_T^{\gamma\gamma}, \tau_{Cj} < 15$ GeV	0	45	120	∞				
	$p_T^{\gamma\gamma}$, 15 GeV $\leq \tau_C^j <$ 25 GeV	0	45	120	∞				
	$p_T^{\gamma\gamma}$, 25 GeV $\leq \tau_C^j <$ 40 GeV	0	120	∞					
	$p_T^{\gamma\gamma}$, 40 GeV $\leq \tau_C^j$	0	200	350	∞				
2-jets Baseline + ≥ 2 jets $p_T^j > 30$ GeV $\|\eta^j\| < 4.7$	$p_T^{j_2}$	30	40	65	90	150	∞		
	$\|y^{j_2}\|$	0.0	0.6	1.2	1.8	2.5	3.5	5.0	
	$\|\Delta\phi_{j_1,j_2}\|$	0.0	0.5	0.9	1.3	1.7	2.5	π	
	$\|\Delta\phi_{\gamma\gamma,j_1j_2}\|$	0.0	2.0	2.7	2.95	3.07	π		
	$\|\bar{\eta}_{j_1j_2} - \eta_{\gamma\gamma}\|$	0.0	0.2	0.5	0.85	1.2	1.7	∞	
	m^{jj}	0	75	120	180	300	500	1000	∞
	$\|\Delta\eta_{j_1j_2}\|$	0.0	0.7	1.6	3.0	5.0	∞		
VBF-enriched 2-jets + $n_{jets} \geq 2$ $\Delta\eta^{jj} > 3.5$ $m^{jj} > 200\,GeV$	$p_T^{\gamma\gamma}$	0	30	60	120	200	∞		
	$p_T^{j_2}$	30	40	65	90	150	∞		
	$\|\Delta\phi_{j_1,j_2}\|$	0.0	0.5	0.9	1.3	1.7	2.5	π	
	$\|\Delta\phi_{\gamma\gamma,j_1j_2}\|$	0.0	2.0	2.7	2.95	3.07	π		

Fiducial cross sections

H→γγ

- **ML unfolding** allows for accounting of bin migrations and correct modeling of systematic uncertainties in all regions of the phase space.
- In $H \to \gamma\gamma$ no explicit regularization procedure was needed, performed **ML unfolding** was sufficient

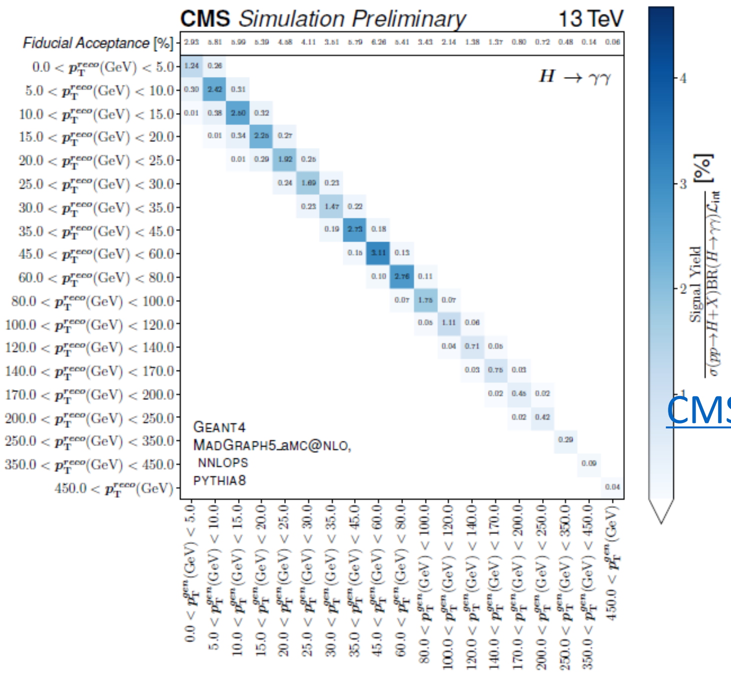

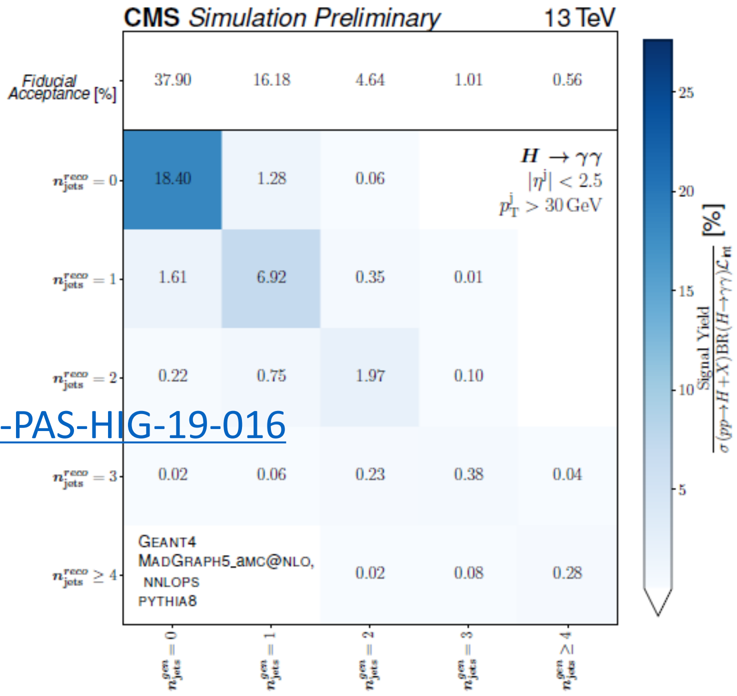

CMS-PAS-HIG-19-016

The event yields divided by the total H→γγ cross-section multiplied by the integrated luminosity for the bins in the **particle-level, reconstruction-level observables** summed across all resolution categories for the **year 2018** for the observables pT and njets are shown

$$\phi_\eta^* = \tan\left(\frac{\phi_{\mathrm{acop}}}{2}\right) \cdot \sin(\theta_\eta^*), \tag{3}$$

where the acoplanarity angle is related to the angle between the particles in the transverse plane as $\phi_{\mathrm{acop}} = \pi - \Delta\phi$, and θ^* is the scattering angle of the two particles with respect to the proton beam in the reference frame in which the two particles are back to back in the (r, θ) plane [54].

Higgs width: a problem difficult to tackle directly!

Total Higgs natural width in SM is small!

- ✓ Too small to be accessed experimentally at LHC from resonance line-shape in analysis where peak can be reconstructed…

Γ_H^{SM} dominated by

$$\Gamma(H \to b\bar{b}) \approx \frac{N_c g_w^2 m_b^2 m_H}{32\pi m_W^2}$$

Γ_H^{SM} = 4.07 MeV

Direct measurement severely limited by detector resolution! One (old) example:

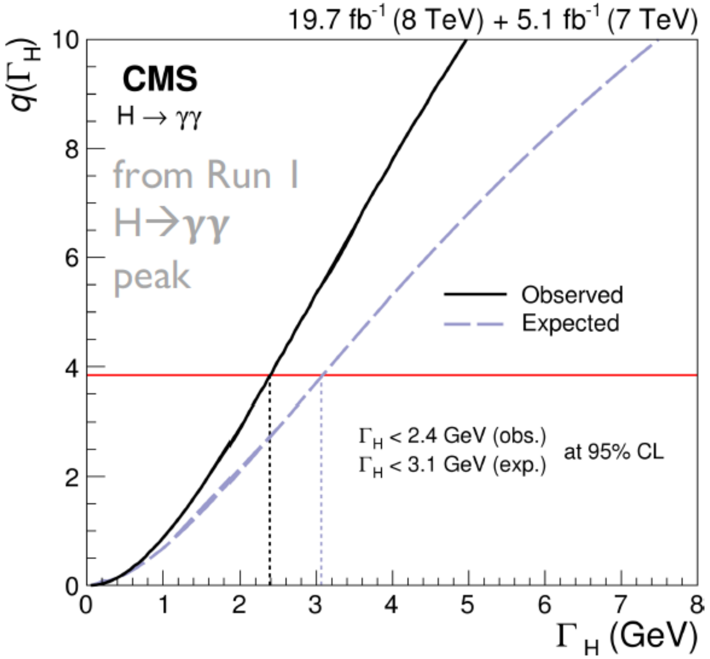

Eur.Phys.J.C 74 (2014) 3076

Γ_H < 2.4 (3.1) GeV obs. (exp.)

H→ ZZ→ 4ℓ : 36 fb^{-1}

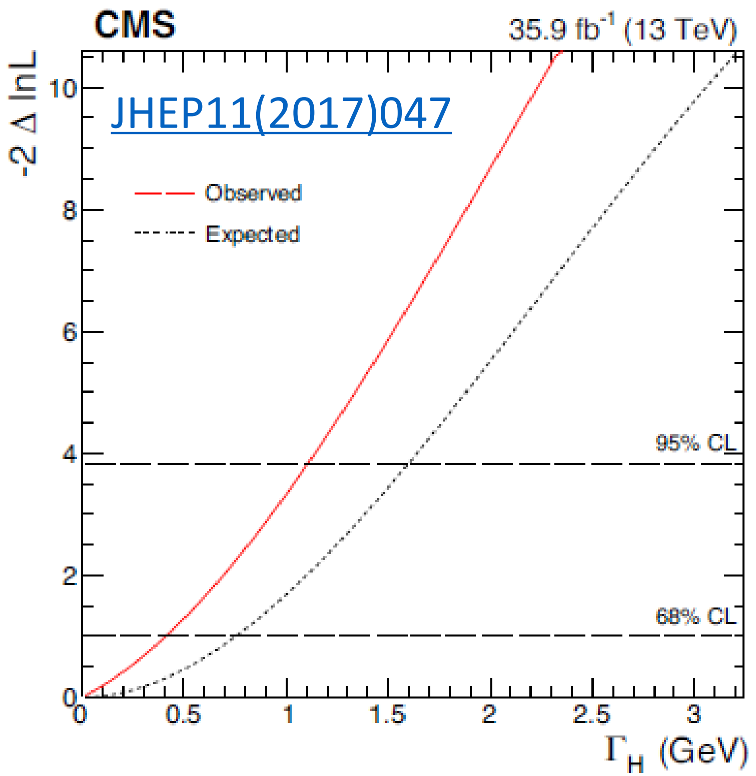

Γ_H < 1.1 (1.6) GeV obs. (exp.) at 95% CL

H→ZZ→4ℓ mass and width projections at HL-LHC

Systematic uncertainty	Baseline	Optimistic	Pessimistic	YR
Muon momentum scale	0.01%	0.005%	0.01%	0.05%
Electron momentum scale	0.15%	0.05%	0.15%	0.10-0.30%
Lepton momentum resolution	10%	5%	10%	5%

$m_{4\ell}$ expected uncertainty (MeV)	inclusive	Rel. Improvement
Total	30	-
Syst impact	20	+33%
Stat only		
N-2D'_{VXBS}	22	-4%
N-1D'_{VXBS}	23	-8%
1D'_{VXBS}	25	-8%
1D_{VXBS}	27	-7%
1D	29	-

Table 3: Expected Higgs boson mass measurement uncertainty, given in MeV, in the inclusive final state.

$m_{4\ell}$ expected uncertainty (MeV)	4μ	4e	2e2μ	2μ2e
Total	32	206	107	112
Syst impact	15	189	94	95
Stat only				
N-2D'_{VXBS}	28	83	51	59
N-1D'_{VXBS}	30	88	53	61
1D'_{VXBS}	32	103	61	68
1D_{VXBS}	34	115	78	71
1D	37	115	78	74

Table 4: Expected Higgs boson mass measurement uncertainty, given in MeV, for the four different final states.

Γ_H expected upper limit (MeV)	inclusive	4μ	4e	2e2μ	2μ2e
Total	177	225	633	362	422
Syst impact	150	188	492	275	323
Stat only	94	124	398	235	272

Table 5: Higgs boson width upper limit at 95% C.L.

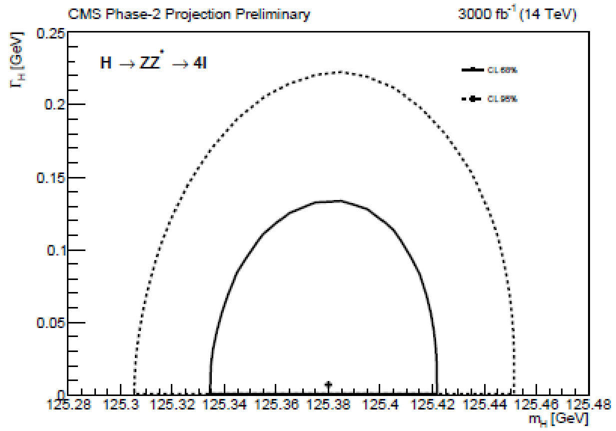

Figure 5: 2D likelihood scan for the Higgs boson width.